

**SYNTHESIS AND CHARACTERIZATION
OF ZnO NANO- AND MICRO- TUBES VIA A FACILE
AQUEOUS SOLUTION PROCESS**

LIWEI LIN

**DOCTOR OF PHILOSOPHY
MATERIALS SCIENCE AND ENGINEERING**



**NAGOYA INSTITUTE OF TECHNOLOGY
JAPAN
MARCH 2009**

名古屋工業大学博士論文

甲第675号(課程修了による)

平成21年3月23日授与

論文題目

簡便な溶液プロセスによる酸化亜鉛ナノおよびマイクロ
チューブの合成とキャラクターゼーション

物質工学専攻博士後期課程

リン リーウェイ

林 黎蔚

指導教員 藤 正督 教授

名古屋工業大学

セラミックス基盤工学研究センター

2009年3月

TABLE OF CONTENTS

CHAPTER 1 GENERAL INTRODUCTION.....	1
1.1 Properties and potential applications of ZnO.....	2
1.2 Crystal structure of ZnO	6
1.3 Typical growth structure of ZnO.....	8
1.4 Synthesis methods of tubular ZnO particles	8
1.5 Objective of this work.....	12
Reference	14
CHAPTER 2 SYNTHESIS OF ZnO MICROTUBES BY INTRODUCING AMMONIA BUBBLES INTO ZINC CHLORIDE AQUEOUS SOLUTION.....	25
2.1 Introduction.....	26
2.2 Origin of design and choice of reagents	27
2.3 Experimental procedure	29
2.3.1 Starting materials	29
2.3.2 Synthesis method	29
2.3.3 Characterization	31
2.4 Effect of the pH on the formation of ZnO microtubes.....	32
2.5 Optimization of drying conditions	40
2.5.1 Open heating system and close heating system	40
2.5.2 Effect of drying temperature	46
2.6 Liquid nitrogen frozen system	52
2.7 Analysis of the particles dried at room temperature	57

2.8 Reaction formula during the synthesis process.....	62
2.9 Transmission Electron Microscopy analysis.....	64
2.10 Conclusion	66
Reference	66
CHAPTER 3 SYNTHESIS OF ZnO NANO- AND MICRO- TUBES USING AMMONIA WATER INSTEAD OF AMMONIA BUBBLES.....	70
3.1 Introduction.....	71
3.2 Experimental procedure	72
3.2.1 Starting materials	72
3.2.2 Synthesis procedure	72
3.2.3 Characterization	75
3.3 Effect of ammonia on the formation of ZnO microtubes	75
3.4 Influence of reaction temperature on the formation of ZnO microtubes	78
3.5 Investigation of aging duration-dependence experiments	81
3.6 Growth mechanism of ZnO microtubes via the aqueous solution process.....	89
3.7 Synthesis of ZnO nanotube.....	92
3.8 Percentage of synthesized ZnO tubes and yield of product.....	95
3.9 Conclusion	97
Reference	98
CHAPTER 4 PHOTOLUMINESCENCE PROPERTY AND X-RAY PHOTOELECTRON SPECTROSCOPY ANALYSIS.....	100
4.1 Introduction.....	101

4.2 Experimental procedure	102
4.3 Results and Discussion	103
4.3.1 Photoluminescence analysis.....	103
4.3.2 X-ray photoelectron spectroscopy (XPS) analysis of ZnO microtubes	107
4.4 Conclusion	112
Reference	113
CHAPTER 5 SUMMARY	115
RESEARCH ACTIVITIES	119
ACKNOWLEDGEMENT	123

CHAPTER 1 GENERAL INTRODUCTION

1.1 Properties and potential applications of ZnO

Zinc oxide (ZnO) is a distinguished material with some special properties, which has attracted intensive research efforts for its unique properties and versatile applications in transparent electronics, ultraviolet (UV) light emitters, piezoelectric devices, chemical sensors and spin electronics in the last few decades. [1-13] ZnO is a wide band-gap (3.37 eV) compound semiconductor that is suitable for short wavelength optoelectronic application. The high exciton binding energy (60 meV) in ZnO crystal can ensure efficient excitonic emission at room temperature and room temperature ultraviolet (UV) luminescence has been reported in disordered particles. The lack of a center of symmetry in wurtzite, combined with large electromechanical coupling, results in strong piezoelectric and pyroelectric properties and the consequent use of ZnO in mechanical actuators and piezoelectric sensors.

Based on these remarkable physical properties and the motivation of device miniaturization, large effort has been focused on the synthesis, characterization and device application of ZnO nano- and micro-materials. ZnO is a versatile functional material that has a diverse group of growth morphologies, such as nanowires, nanorings, nanotetrapods, nanotubes, nanobelts, nanocombs, nanocages, nanopropellers, [14-28] which have been successfully grown via a variety of methods including chemical vapor deposition, thermal evaporation, electrodeposition, etc. These structures have been subjected to electrical transport, UV emission, gas sensing and ferromagnetic doping

studies, and considerable progresses have been achieved. [29]

The above mentioned properties are typically describes a few of them in the followings:

a) Luminescent property

ZnO exhibits a direct band-gap of 3.37 eV at room temperature with a large exciton of 60 mV. The strong exciton binding energy, which is much larger than that of GaN (25 mV), and the thermal energy at room temperature (26 mV) can ensure an efficient exciton emission at room temperature under low excitation energy. As a consequence, ZnO is recognized as a promising photonic material in the blue-UV region. Photoluminescence (PL) spectra of ZnO structures have been extensively reported. [30-35] Excitonic emissions have been observed from the photoluminescence spectra of ZnO nanorods. [36]. Besides UV emitting and lasing, effort on utilizing ZnO nanowires for UV photodetection and optical switching have been reported by King *et al.* [37]

b) Gas and chemical sensors

Conductometric metal oxide semiconductor thin films are the most promising among solid state chemical sensors, due to their small dimension, low cost, low power consumption, on-line operation and high compatibility with microelectronic processing. The fundamental sensing mechanism of metal oxide based gas sensors relies on a change in electrical conductivity due to the process of interaction between the surface complexes, such as O^- , O_2^- , H^+ and OH^- reactive chemical species and the gas molecules

to be detected. Oxygen vacancies on metal-oxide surface are electrically and chemically active. These vacancies function as *n*-type donors often significantly increase the conductivity of oxide. Upon adsorption of charge accepting molecules at the vacancy sites, such as NO₂ and O₂, electrons are effectively depleted from the conduction band, leading to a reduced conductivity of the *n*-type oxide. On the other hand, molecules, such as CO and H₂, would react with surface adsorbed oxygen and consequently remove it, leading to an increase of conductivity. As one of the major materials for solid state gas sensor, bulk and thin films of ZnO have been proposed for CO [38, 39], NH₃ [40], alcohol [41] and H₂ [42].

c) Piezoelectric effect and polar surfaces

As one of the important properties of ZnO, its piezoelectricity has been extensively studied for various applications in force sensing, acoustic wave resonator, acousto-optic modulator, *etc.* [43-50] Piezoelectricity is due to atomic scale polarization. To illustrate the piezoelectricity, one considers an atom with positive charge that is surrounded tetrahedrally by anions, as shown in Figure 1.1. [51] The center of gravity of the negative charges is at the centre of the tetrahedron. On exerting a pressure on the crystal along the cornering direction of the tetrahedron, the tetrahedron will experience a distortion and the center of gravity of the negative charges will no longer coincide with the position of the positive central atom; an electric dipole is generated. If all of the tetrahedral in the crystal have the same orientation or some other mutual orientation that

does not allow for a cancellation among the dipoles, the crystal will have a macroscopic dipole. The two opposite faces of the crystal have opposite electric charges.

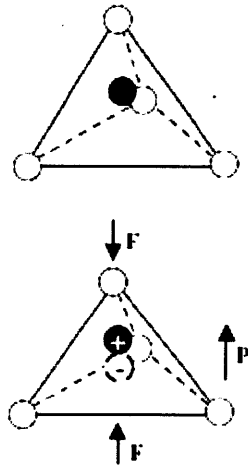


Figure 1.1 Schematic diagrams showing the piezoelectric effect in a tetrahedrally coordinated cation–anion unit

Another interesting result of the non-centrosymmetric ZnO crystal structure is its spontaneous polarization and polar face dominated nanostructure. [52-54] As mentioned before, the crystal structure of ZnO can be visualized in a way that oxygen atoms and zinc atoms are tetrahedrally bonded. These tetrahedrons stack along [0001] direction. Due to spontaneous polarization, the position of positive charge is displaced from that of negative charge and the direction of displacement is also [0001]. The net result of this spontaneous polarization is a charged (0001) surface. In order to achieve minimized energy, the charged (0001) surface results in unique nano-ring and nano-coil structure. [6]

1.2 Crystal structure of ZnO

Wurtzite zinc oxide has a hexagonal structure (space group $C6mc$) with lattice parameters $a = 0.3296$ and $c = 0.52065$ nm. The structure of ZnO can be simply described as a number of alternating planes composed of tetrahedrally coordinated O^{2-} and Zn^{2+} ions, stacked alternately along the c -axis (Figure 1.2). [55] The tetrahedral coordination in ZnO results in noncentral symmetric structure and consequently piezoelectricity and pyroelectricity. Another important characteristic of ZnO is polar surface. To maintain a stable structure, the polar surfaces generally have facets or exhibit massive surface reconstructions, but ZnO_{\pm} (0001) are exceptions: they are atomically flat, stable and without reconstruction. [56, 57]

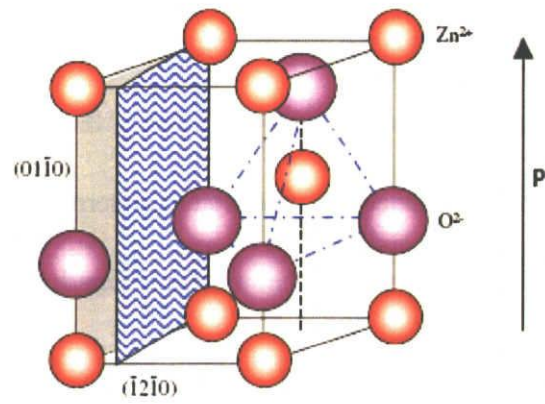


Figure 1.2 The wurtzite structure model of ZnO (The tetrahedral coordination of Zn-O is shown.)

1.3 Typical growth structure of ZnO

Structurally, ZnO has three types of fast growth directions: $\langle 2\bar{1}\bar{1}0 \rangle$ ($\pm [2\bar{1}\bar{1}0]$, $\pm [\bar{1}2\bar{1}0]$, $\pm [\bar{1}\bar{1}20]$); $\langle 01\bar{1}0 \rangle$ ($\pm [01\bar{1}0]$, $\pm [10\bar{1}0]$, $\pm [1\bar{1}00]$); and $\pm [0001]$. Together with the polar surface due to atomic terminations, ZnO exhibits a wide range of unique structures that can be grown by tuning the growth rates along these directions. These are the fundamental principles understanding the formation of numerous ZnO morphologies. One of the most profound factors determining the morphology involves the relative surface activities of various growth facets under given conditions. Macroscopically, a crystal has different kinetic parameters for different crystal planes, which are emphasized under controlled growth conditions. Thus, after an initial period of nucleation and incubation, a crystallite will commonly develop into a three-dimensional object with well-defined, low index crystallographic faces. These structures tend to maximize the areas of the $\{2\bar{1}\bar{1}0\}$ and $\{01\bar{1}0\}$ facets because of the lower energy.

1.4 Synthesis methods of tubular ZnO particles

Besides nanowires, nanobelts and nanorods, other complex ZnO nanostructures such as tubular ZnO particles [58-62] also attract considerable research interests. Since the discovery of carbon nanotube [63], several methods for fabrication of ZnO particles

with tubular structure have been reported, such as vapor phase depositions, thermal oxidation, a template-assisted method and a hydrothermal process. A few of them are described in the followings:

A) The most common method synthesize ZnO nanostructure utilizes a vapor transport process. [64-66] In such a process, zinc or zinc oxide and oxygen or oxygen mixture vapor are transported and react with each other, forming ZnO nanostructure. According to the difference on the formation mechanisms, the extensively used vapor transport process can be categorized into the catalyst free vapor-solid (VS) process [67, 68] and catalyst assisted vapor-liquid-solid (VLS) process [69, 70]. The typical process is usually carried out in a horizontal tube furnace, as shown in Figure 1.3 [51], which is composed of a horizontal tube furnace, an alumina tube, a rotary pump system and a gas supply and control system. R.M. Wang has synthesized ZnO nanotubes through heating the mixture of Zn and ZnO powder at 1300 °C in Ar flow. [71]

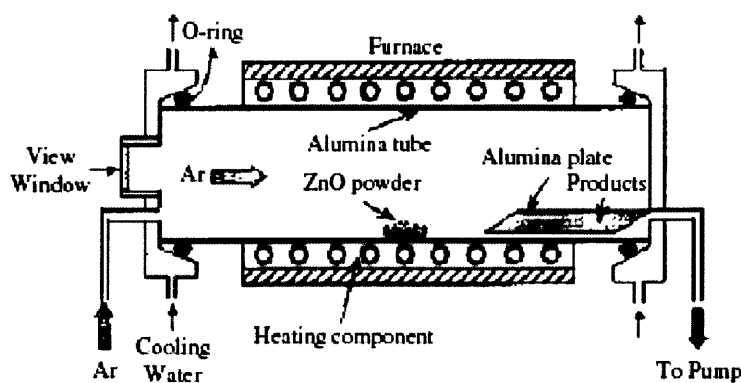


Figure 1.3 A schematic diagram of the experimental apparatus by the vapor transport process

B) Another evaporating synthesis method to synthesize ZnO particles is metal-organic chemical vapor deposition. [72] The typical diagrammatic sketch of metal-organic chemical vapor deposition (MOCVD) device system is shown in Figure 1.4. [73] In a typical CVD process, the substrate is exposed to the volatile precursor, which reacts or decomposes on the substrate surface to produce the high purity, high performance film. Frequently, volatile by-products are also produced, which are removed by gas flow through the reaction chamber. Through CVD method, the steams of volatile metal compounds or metal organic compounds is used as raw materials, and through chemical reaction made into the material needed. Then it condenses rapidly under protection of inert gases for preparation of particles. The ZnO particles prepared by CVD possess high purity, uniform particle size which can be accurately controlled. B. P. Zhang et al [74] have reported that ZnO tubes were epitaxially grown on sapphire (0001) substrate by MOCVD. The growth pressure and temperature were 0.3-3 Torr and 475 °C, separately. Oxygen gas and diethyl zinc were used as precursors and nitrogen gas was used as the carrier gas for DEZn by-product.

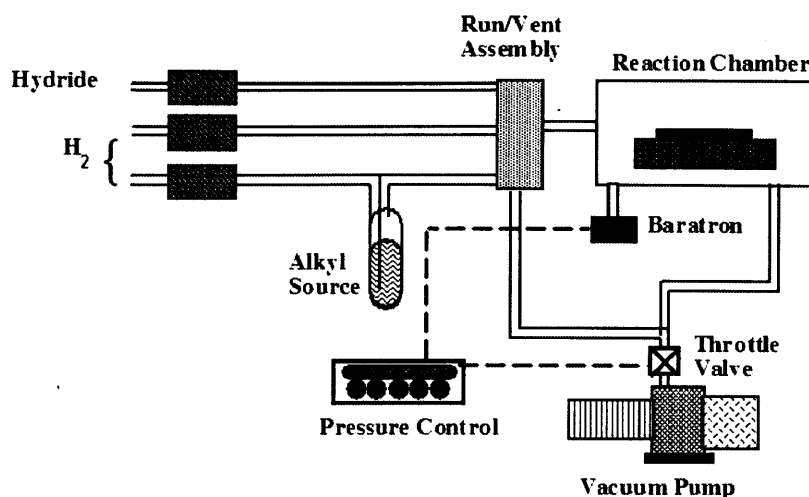


Figure 1.4 Diagrammatic sketch of atmospheric metal-organic chemical vapor deposition (MOCVD) device system

C) Other synthesis methods

Although the vapor transport process and hydrothermal method are the dominant synthesis processes for synthesis ZnO particles with tubular structure. Other growth methods such as hydrothermal methods [75-80], replication and template techniques [81-85] and laser patterning [86] have been developed in parallel. These methods provide the possibility of forming ZnO tubes at low temperature. For example, via a hydrothermal method [76], Vayssieres et al. have reported the synthesis of ZnO microtubes, on a range of substrates, immersed in a bottle with an autoclavable screw cap containing equimolar amounts of zinc nitrate and hexamethylenetetramine and maintained at 90 °C for 2 days. Z. Wang and H. L. Li [84] have synthesized ZnO

nanotubes via a sol-gel process within the pores of an anodic aluminum oxide (AAO) template.

Rigid experimental conditions (such as high temperature), sophisticated equipments (such as autoclave), and complex procedure were usually employed in the above mentioned methods in order to obtain single-crystalline and high purity ZnO tubes. Furthermore, most of the reported approaches produced ZnO tubes in small quantities and high cost, restricting their commercial applications. So it is necessary to develop a template-free and surfactant-free method at low temperature, low cost and normal pressure.

1.5 Objective of this work

The objective of this work is to develop a new and facile method to synthesize ZnO particles with tubular structure and to focus on the influence of external parameters such as reaction temperature, pH because of their importance for the formation of ZnO microtubes. Our developed method has some advantages, such as synthesis under atmospheric pressure at a common 500 ml glass flask, which is located in a water bath kept at different temperature, low cost and easy control. The growth mechanism of ZnO microtubes has been of particular interest. Also of interest has been the development of the microstructure of ZnO particles, with focus on the morphological evolution during the synthesis process.

The thesis is organized as follows:

In chapter 2, first introduce the design of this method, which mainly include the choice of reagents. Then using the developed method, hexagonal ZnO microtubes were successfully synthesized via an aqueous solution process through the introduction of ammonia bubbles into zinc chloride solution. The influence of the final pH value on the formation of ZnO microtubes was discussed. And the optimization of drying process was systematically carried out. From this research, it can be get that the ammonia bubbles is not the template for the formation of ZnO microtubes, but just as the reactant, which step further in proposing the formation mechanism.

In chapter 3 investigated the synthesis of ZnO microtubes using the ammonia water instead of ammonia bubbles in the aqueous solution, which is easier to control. The effects of ammonia and reaction temperature were discussed in this chapter. In order to get the evidence of the intermediate morphologies, systematical aging duration-dependent experiments were compared comprehensively to reveal the formation and detailed growth process of ZnO particles with tubular structure. Based on the results and the special ZnO crystal property, the mechanism of the formation of ZnO tubes was proposed. Also, through adjusting the reaction temperature, aging time and temperature, the starting concentration of zinc ions, ZnO nanotubes were successfully fabricated via the developed aqueous solution method.

In chapter 4, the synthesized ZnO microtubes were investigated by photoluminescence (PL) analysis and X-ray photoelectron spectroscopy (XPS). These

studies have investigated PL characteristics of ZnO tubes based on the analyses of XPS.

Finally, in chapter 5, the concluding remarks of the present work were stated.

Reference

- [1] K. Nomura, H. Ohta, K. Ueda, T. Kamiya, M. Hirano, and H. Hosono, "Thin-film transistor fabricated in single-crystalline transparent oxide semiconductor", *Science* 300 (2003) 1269-1272.
- [2] T. Nakada, Y. Hirabayashi, T. Tokado, D. Ohmori, and T. Mise, *Sol. Energy*, 77 (2004), 739.
- [3] S. Y. Lee, E. S. Shim, H. S. Kang, S. S. Pang, and J. S. Kang, "Fabrication of ZnO thin film diode using laser annealing", *Thin Solid Films*, 437 [1] (2005), 31-34.
- [4] R. Könenkamp, R. C. Word, and C. Schlegel, "Vertical nanowire light-emitting diode", *Appl. Phys. Lett.*, 85 (2004), 6004-6006.
- [5] S. T. McKinstry, and P. Muralt, *J. Electroceram.*, 12 (2004), 7.
- [6] Z. L. Wang, X. Y. Kong, Y. Ding, P. Gao, W. L. Hughes, R. Yang, and Y. Zhang, "Semiconducting and Piezoelectric Oxide Nanostructure Induced by Polar Surface", *Adv. Funct. Mater.*, 14 (2004), 943-956.
- [7] M. S. Wagh, L. A. Patil, T. Seth, and D. P. Amalnerkar, "Surface cupricated SnO₂-ZnO thick films as a H₂S gas sensor", *Mater. Chem. Phys.*, 84 (2004), 228-233.

- [8] Y. Ushio, M. Miyayama, and H. Yanagida, "Effects of interface states on gas-sensing properties of a CuO/ZnO thin-film heterojunction", *Sensor Actuat. B*, 17 (1994), 221-226.
- [9] H. Harima, "Raman studies on spintronics materials based on wide bandgap semiconductors", *J. Phys.: Condens. Matter* 16 (2004), S5653-S5660.
- [10] S. J. Pearton, W. H. Heo, M. Ivill, D. P. Norton, and T. Steiner, "Dilute Magnetic Semiconducting Oxides", *Semicond. Sci. Technol.*, 19 (2004), R59-74.
- [11] J. Nishii, F.M. Hossain, S. Takagi, T. Aita, K. Saikusa, Y. Ohmaki, I. Ohkubo, S. Kishimoto, A. Ohtomo, T. Fukumura, F. Matsukura, Y. Ohno, H. Koinuma, H. Ohno, and M. Kawasaki, "High Mobility Thin Film Transistors with Transparent ZnO Channels", *Jpn. J. Appl. Phys.*, 42 (2003), L347-349.
- [12] F. M. Hossain, J. Nishii, S. Takagi, T. Sugihara, A. Ohtomo, T. Fukumura, H. Koinuma, H. Ohno, M. Kawasaki, "Modeling of grain boundary barrier modulation in ZnO invisible thin film transistors", *Physica E*, 21 (2004), 911-915.
- [13] Q. H. Li, Y. X. Liang, Q. Wan, T. H. Wang, "Oxygen sensing characteristics of individual ZnO nanowire transistors", *Appl. Phys. Lett.*, 85 (2004), 6389-6391.
- [14] Greyson E. C., Babayan Y., Odom T. W., "Directed Growth of Ordered Arrays of Small-Diameter ZnO Nanowires", *Adv. Mater.*, 16 (2004), 1348-1352.
- [15] Z. X. Pan, Z. R. Dai, Z. L. Wang, "Nanobelts of Semiconducting Oxides", *Science*, 291 (2001), 1947-1949.
- [16] P. X. Gao, Z. L. Wang, "Nanopropeller arrays of zinc oxide", *Appl. Phys. Lett.*, 84

- (2004), 2883-2885.
- [17] P. X. Gao, Z. L. Wang, "Mesoporous Polyhedral Cages and Shells formed by Textured Self-assembly of ZnO Nanocrystals", *J. Am. Chem. Soc.*, 125 (2003), 11299-11305.
- [18] Y. Sun, G. M. Fuge, N. A. Fox, D. J. Riley, M. N. R. Ashfold, "Synthesis of aligned arrays of ultrathin ZnO nanotubes on a Si wafer coated with a thin ZnO film", *Adv. Mater.*, 17 (2005), 2477-2481.
- [19] S. W. Kim and S. Fujita, "ZnO nanowires with high aspect ratios grown by metalorganic chemical vapor deposition using gold nanoparticles", *Appl. Phys. Lett.*, 86 (2005), 153119.
- [20] H. Zhou and Z. Li, "Synthesis of nanowires, nanorods and nanoparticles of ZnO through modulating the ratio of water to methanol by using a mild and simple solution method", *Mater. Chem. Phys.*, 89 (2005), 326-331.
- [21] D. W. Zeng, C. S. Xie, M. Dong, R. Jiang, X. Chen, A. H. Wang, J. B. Wang, and J. Shi, "Spinel-type ZnSb₂O₄ nanowires and nanobelts synthesized by an indirect thermal evaporation", *Appl. Phys. A*, 79 (2004), 1865-1868.
- [22] J. Zhang, L. D. Sun, X. C. Jiang, C. S. Lian, and C. H. Yan, "Shape Evolution of One-Dimensional Single-Crystalline ZnO Nanostructures in a Microemulsion System" *Cryst. Growth Des.*, 4 (2004), 309-313.
- [23] H. Zhang, D. Yang, X. Ma, Y. Ji, J. Xu, and D. Que, "Synthesis of flower-like ZnO nanostructures by an organic-free hydrothermal process", *Nanotechnology* 15 (2004), 622-626.

- [24] P. X. Gao and Z. L. Wang, "Substrate Atomic-Termination-Induced Anisotropic Growth of ZnO Nanowires/Nanorods by the VLS Process", *J. Phys. Chem. B*, 108 (2004), 7534-7537.
- [25] Y. H. Leung, A. B. Djurišić, J. Gao, M. H. Xie, Z. F. Wei, S. J. Xu, and W. K. Chan, "Zinc oxide ribbon and comb structures: synthesis and optical properties", *Chem. Phys. Lett.*, 394 (2004), 452-457.
- [26] F. Liu, P. J. Cao, H. R. Zhang, J. Q. Li, and H. J. Gao, "Controlled self-assembled nanoaeroplanes, nanocombs, and tetrapod-like networks of zinc oxide", *Nanotechnology*, 15 (2004), 949-952.
- [27] P. A. Hu, Y. Q. Liu, L. Fu, X. B. Wang, D. B. Zhu, "Creation of novel ZnO nanostructures: self-assembled nanoribbon/nanoneedle junction networks and faceted nanoneedles on hexagonal microcrystals", *Appl. Phys. A*, 78 (2004), 15-19.
- [28] Z. R. Tian, J. A. Voigt, J. Liu, B. Mckenzie, M. J. Mcdermott, "Complex and oriented ZnO nanostructures", *Nat. Mater.*, 2 (2003), 821-826.
- [29] Z. Fan and J. G. Lu, "Nanostructured ZnO : Building blocks for nanoscale devices", *International Journal of High Speed Electronics and Systems*, 16 [4] (2006), 883-896.
- [30] K. Vanheusden, W. L. Warren, C. H. Seager, D. R. Tallant and J. A. Voigt, "Mechanisms behind green photoluminescence in ZnO phosphor powders", *J. Appl. Phys.*, 79 [10] (1996), 7983-7990.

- [31] X. J. Yang, X. Y. Miao, X. L. Xu, C. M. Xu, J. Xu, H. T. Liu, "Structure, X-ray photoelectron spectroscopy and photoluminescence properties of highly ordered ZnO microrods", *Opt. Mater.*, 27 (2005), 1602-1605.
- [32] Le Hong Quang, Soo Jin Chua, Kian Ping Loh, Eugene Fitzgerald, "The effect of post-annealing treatment on photoluminescence of ZnO nanorods prepared by hydrothermal synthesis", *J. Cryst. Growth*, 287 (2006), 157-161.
- [33] D. F. Liu, D. S. Tang, L. J. Ci, X. Q. Yan, Y. X. Liang, Z. P. Zhou, H. J. Yuan, W. Y. Zhou, G. Wang, "Synthesis and Strong Blue-Green Emission Properties of ZnO Nanowires", *Chin. Phys. Lett.*, 20 (2003), 928-931.
- [34] H. J. Fan, R. Scholz, F. M. Kolb, M. Zacharias, U. Gösele, F. Heyroth, C. Eisenschmidt, T. Hempel, "On the growth mechanism and optical properties of ZnO multi-layer nanosheets", *J. Christen, Appl. Phys. A*, 79 (2004), 1895-1990.
- [35] T. W. Kim, T. Kawazoe, S. Yamazaki, M. Ohtsu, and T. Sekiguchi, "Low-temperature orientation-selective growth and ultraviolet emission of single-crystal ZnO nanowires", *Appl. Phys. Lett.*, 84 (2004), 3358-3360.
- [36] W.I. Park, Y.H. Jun, S.W. Jung, and G. Yi, *Appl. Phys. Lett.*, "Excitonic emissions observed in ZnO single crystal nanorods", 82 (2003), 964-966.
- [37] Y. Gu, I. L. Kuskovsky, M. Yin, S. O'Brien, and G. G. Neumark, "Quantum confinement in ZnO nanorods", *Appl. Phys. Lett.*, 85 (2004), 3833-3835.
- [38] J. X. Wang, X. W. Sun, H. Huang, Y. C. Lee, O. K. Tan, M. B. Yu, G. Q. Lo, D. L. Kwong, "A two-step hydrothermally grown ZnO microtube array for CO gas

- sensing”, *Appl. Phys. A*, 88 [4] (2007), 611-615.
- [39] H. W. Ryu, B. S. Park, S. A. Akbar, W. S. Lee, K. J. Hong, Y. Jin Seo, D. C. Shin, J. S. Park, G. P. Choi, “ZnO sol-gel derived porous film for CO gas sensing”, *Sens. Actuator B*, 96 (2003), 717-722.
- [40] G. Sberveglieri, “Recent developments in semiconducting thin-film gas sensors”, *Sens. Actuator B*, 23 (1995), 103-109.
- [41] G. S. Trivikrama Rao, D. Tarakarama Rao, “Gas sensor response of ZnO based thick film sensor to NH₃ at room temperature”, *Sens. Actuator B*, 55 (1999), 166-169.
- [42] X. L. Cheng, H. Zhao, L. H. Huo, S. Gao, J. G. Zhao, “ZnO nanoparticulate thin film: preparation, characterization and gas-sensing property”, *Sens. Actuator B*, 102 (2004), 248-252.
- [43] M. Catti, Y. Noel, and R. Dovesi, *J. Phys. Chem. Solids*, “Full piezoelectric tensors of wurtzite and zinc blende ZnO and ZnS by first-principles calculations”, 64 (2003), 2183-2190.
- [44] A. D. Corso, M. Posternak, R. Resta, and A. Baldereschi, “Ab initio study of piezoelectricity and spontaneous polarization in ZnO”, *Phys. Rev. B*, 50 [15] (1994), 10715-10721.
- [45] J. G. E. Gardeniers, Z. M. Rittersma, and G. J. Burger, “Preferred orientation and piezoelectricity in sputtered ZnO films”, *J. Appl. Phys.*, 83 (1998), 7844-7854.
- [46] J. Molarius, J. Kaitila, T. Pensala, and M. Ylilammi, “Piezoelectric ZnO films by

- r.f. sputtering”, *J. Mater. Sci.: Mater. Electron.*, 14 (2003), 431-435.
- [47] C. R. Wuethrich, C. A. P. Muller, G. R. Fox, and H. G. Limberger, “All-fiber acousto-optic modulator using ZnO piezoelectric actuators”, *Sensor Actuat. A*, 66 (1998), 114-117.
- [48] T. Itoh, and T. Suga, “Force sensing microcantilever using sputtered zinc oxide thin film”, *Appl. Phys. Lett.*, 64 (1994), 37-39.
- [49] R. Paneva, G. Temmel, E. Burte, and H. Ryssel, “Micromechanical ultrasonic liquid nebulizer”, *Sensor Actuat. A*, 62 (1997), 765-767.
- [50] A R. Hutson, “Piezoelectricity and Conductivity in ZnO and CdS”, *Phys. Rev. Lett.* 4 (1960), 505-506.
- [51] Z. L. Wang, “Zinc oxide nanostructures: growth, properties and applications”, *J. Phys. Condens. Matter*, 16 (2004), 829-858.
- [52] X. Y. Kong, Z. L. Wang, “Spontaneous polarization-induced nanohelices, nanosprings, and nanorings of piezoelectric nanobelts”, *Nano. Lett.*, 3 (2003), 1625-1631.
- [53] X. Y. Kong, Y. Ding, R. Yang, and Z. L. Wang, “Single-crystal nanorings formed by epitaxial self-coiling of polar-nanobelts”, *Science* 303 (2004), 1348-1351.
- [54] X. Y. Kong, and Z. L. Wang, “Polar-surface dominated ZnO nanobelts and the electrostatic energy induced nanohelices/nanosprings”, *Appl. Phys. Lett.*, 84 (2004), 975-977.
- [55] P. X. Gao and Z. L. Wang, “Nanoarchitectures of semiconducting and piezoelectric

zinc oxide”, *J. Appl. Phys.*, 97 (2005), 044304.

- [56] Dulub O., Boatner L. A. and Diebold U., “STM study of the geometric and electronic structure of ZnO(0 0 0 1)-Zn, (0 0 0 1)-O, (1 0 1 0), and (1 1 2 0) surfaces”, *Surf. Sci.*, 519 (2002), 201-217.
- [57] Meyer B. and Marx D., “Density-functional study of the structure and stability of ZnO surfaces”, *Phys. Rev. B*, 67 (2003), 035403.1-035403.11.
- [58] X. H. Kong and Y. D. Li, “Ultraviolet-emitting ZnO microtube array synthesized by a catalyst-assisted flux method”, *Chem. Lett.*, 32 [11] (2003), 1162-1163.
- [59] J. X. Duan, X. T. Huang and E. K. Wang, *Mater. Lett.*, “PEG-assisted synthesis of ZnO nanotubes”, 60[15] (2006), 1918-1921.
- [60] J. Zhou, Z. D. Wang, L. Wang, M. Wu, S. X. Ouyang, E. Gu, “Synthesis of ZnO hexagonal tubes by a microwave heating method”, *Superlattice Microst.*, 39 (2006), 314-318.
- [61] L. G. Yu, G. M. Zhang, S. Q. Li, Z. H. Xi, D. Z. Guo, “Fabrication of arrays of zinc oxide nanorods and nanotubes in aqueous solution under an external voltage”, *J. Cryst. Growth*, 299 (2007), 184-188.
- [62] B. Y. Geng, X. W. Liu, X. W. Wei, S. W. Wang, “Large-scale synthesis of single-crystalline ZnO nanotubes based on polymer-inducement”, *Mater. Res. Bull.*, 41 [10] (2006), 1979-1983.
- [63] S. Iijima, “Helical microtubules of graphitic carbon *Nature*”, 354 (1991), 56-58.
- [64] P. Chang, Z. Fan, W. Tseng, D. Wang, W. Chiou, J. Hong, J. G. Lu, “ZnO

- Nanowires Synthesized by Vapor Trapping CVD Method”, *Chem. Mater.*, 16 [24] (2004), 5133-5137.
- [65] B. P. Zhang, N. T. Binh, K. Wakatsuki, Y. Segawa, Y. Kashiwaba, and K. Haga, “Synthesis and optical property of single crystal ZnO nanorods”, *Nanotechnology*, 15 (2004), 382-388.
- [66] Shisheng Lin, Zhizhen Ye, Haiping He, Binghui Zhao, Liping Zhu, and Jingyun Huang, “Photoluminescence properties of ZnO nanoneedles grown by metal organic chemical vapor deposition”, *J. Appl. Phys.*, 104 (2008), 064311.
- [67] H. J. Fan, F. Bertram, A. Dadgar, J. Christen, A. Krost, and M. Zacharias, “ Self-assembly of ZnO nanowires and the spatial resolved characterization of their luminescence”, *Nanotechnology*, 15 (2004), 1401-1404.
- [68] Y. K. Tseng, C. T. Chia, C. Y. Tsay, L. J. Lin, H. M. Cheng, C. Y. Kwo, and I. C. Chen, “Growth of epitaxial needle-like ZnO nanowires on GaN films”, *J. Electrochem. Soc.*, 152 (2005), 95-98.
- [69] H. Chik, J. Liang, S. G. Cloutier, N. Kouklin, J. M. Xu, “ Periodic array of uniform ZnO nanorods by second-order self-assembly”, *Appl. Phys. Lett.*, 84 (2004), 3376-3378.
- [70] H. J. Fan, F. Fleischer, W. Lee, K. Nielsch, R. Scholz, M. Zacharias, U. Gösele, A. Dadgar and A. Krost, “ Patterned growth of aligned ZnO nanowire arrays on sapphire and GaN layers”, *Supperlattice Microst.*, 36 (2004), 95-105.
- [71] R. M. Wang, Y. J. Xing, J. Xu and D. P. Yu, “Fabrication and microstructure

- analysis on zinc oxide nanotubes”, *New J. Phys.*, 5 (2003), 115.1-115.7.
- [72] X.L. Yuana, B.P. Zhangb, J. Niitsumaa, T. Sekiguchia, “Cathodoluminescence characterization of ZnO nanotubes grown by MOCVD on sapphire substrate”, *Mat. Sci. Semicon. Proc.*, 9 (2006), 146–150.
- [73] http://en.wikipedia.org/wiki/Metalorganic_vapour_phase_epitaxy
- [74] B. P. Zhang, N. T. Binh, K. Wakatsuki, Y. Segawa, Y. Yamada, N. Usami, M. Kawasaki, H. Koinuma, “Formation of highly aligned ZnO tubes on sapphire (0001) substrates”, *Appl. Phys. Lett.*, 84 (2004), 4098-4100.
- [75] Y. Y. Ding, Z. Gui, J. X. Zhu, S. S. Yan, J. Liu, Y. Hu, Z. Z. Wang, “Fabrication of tubular ZnO by vesicle-template fusion”, *Mater. Lett.*, 61 (2007), 2195-2199.
- [76] Vayssieres L., Keis K., Hagfeldt A., Lindquist S. E., “Three-dimensional array of highly oriented crystalline ZnO microtubes”, *Chem. Mater.*, 13 (2001), 4395-4398.
- [77] H. D. Yu, Z. P. Zhang, M. Y. Han, X. T. Hao, F. F. Zhu, “A general low-temperature route for large-scale fabrication of highly oriented ZnO nanorod/nanotubes arrays”, *J. Am. Chem. Soc.*, 127 (2005), 2378-2379.
- [78] Q. C. Li, V. Kumar, Y. Li, H. T. Zhang, T. J. Marks, R. P. H. Chang, “Fabrication of ZnO nanorods and nanotubes in aqueous solutions”, *Chem. Mater.*, 17 (2005), 1001-1006.
- [79] A. L. Yang and Z. L. Cui, “ZnO layer and tubular structures synthesized by a simple chemical solution route”, *Mater. Lett.*, 60 [19] (2006), 2403-2405.
- [80] Y. H. Tong, Y. C. Liu, C. L. Shao, Y. X. Liu, C. S. Xu, J. Y. Zhang, Y. M. Lu, D. Z.

- Shen and X. W. Fan, "Growth and optical properties of faceted hexagonal ZnO nanotubes", *J. Phys. Chem. B*, 110 (2006), 14714-14718.
- [81] B.I. Seo, U.A. Shaislamov, M.H. Ha, S.-W. Kim, H.-K. Kim and Beelyong Yang, "ZnO nanotubes by template wetting process", *Physica E, Proceedings of the E-MRS 2006 Symposium E: Science and Technology of Nanotubes and Nanowires*, 37 [1-2] (2007), 241-244.
- [82] Cepak V.M., Hulteen J.C., Che G., Jirage K.B., Lakshmi B.B., Fischer E.R., Martin C.R., "Chemical strategies for template syntheses of composite micro- and nanostructure", *Chem. Mater.*, 9 [5] 1997, 1065-1067.
- [83] Terrones M., Grobert N., Olivares J., Zhang J.P., Terrones H., Kordatos K., Hsu W.K., Hare J.P., Townsend P.D., Prassides K., Cheetham A.K., Kroto H.W., Walton D.R.M., "Controlled production of aligned-nanotubes bundles", *Nature*, 388 1997, 52-55.
- [84] Z. Wang, H. L. Li, "Highly ordered zinc oxide nanotubules synthesized within the anodic aluminum oxide template", *Appl. Phys. A*, 74 (2002), 201-203.
- [85] M. Lai, D. J. Riley, "Templated Electrosynthesis of Zinc Oxide Nanorods", *Chem. Mater.*, 18 (2006), 2233-2237.
- [86] Nanai L., George T.F., "Laser-assisted formation of metallic oxide microtubes", *J. Mater. Res.*, 12 [1] 1997, 283-284.

**CHAPTER 2 SYNTHESIS OF ZnO MICROTUBES BY
INTRODUCING AMMONIA BUBBLES INTO ZINC
CHLORIDE AQUEOUS SOLUTION**

2.1 Introduction

ZnO particles with tubular structure have been achieved through various techniques, such as thermal evaporation [1-3], solid-vapor synthetic approach [4], and microwave plasma system [5]. In contrast to the physical methods, chemical methods, such as hydrothermal method [6,7], polymer-induced method [8], PEG-assisted synthesis [9], have shown distinct advantages for the synthesis of tubular ZnO particles, which can be carried out at low temperature, under atmospheric pressure, and could produce ZnO particles in large-scale quantities. Chemical methods, including precipitation from inorganic or organic solutions and sol-gel techniques can conveniently provide control of nucleation, growth and aging of particles in the solution. The methods rely on advanced solution and coordination chemistry theories enabling the synthesis of the required precursor particles utilizing a variety of parameters to enable control of the formation process.

In this chapter, a similar but simplified and facile process has been developed to synthesize the hexagonal ZnO microtubes in a large scale by a low cost aqueous solution method. In comparison with other previous studies, we did not introduce any other chemicals except reactants in the reaction solution. Besides this, the advantages of our utilizing-aqueous solution-based method are template-free, surfactant-free, and performed in a glass flask under ambient pressure and relative low temperature. The original experiment's design is to use the ammonia bubbles as the template of ZnO

microtubes. The function of ammonia bubbles is not only the reactant but also the template.

2.2 Origin of design and choice of reagents

The original design is from the developed new approach to synthesize hollow calcium carbonate particles, which is involved the mixed gas (CO_2+N_2) as bubbles templates. The advantage of this new approach is to simplify the synthesis of hollow particles by leaving out the removal of template. [10-12] Therefore, this method is carried out for the synthesis of hollow ZnO particles, which are introduced ammonia bubbles into zinc ions aqueous solution. The function of ammonia bubbles is used as not only the reactant but also the template.

In order to choose a suitable zinc ions aqueous solution, 0.5 M zinc chloride aqueous solution and 0.5 M zinc sulfate aqueous solution were prepared, separately. And then ammonia bubbles were introduced into these two kinds of zinc ions aqueous solution, which is kept in a water bath for 90 °C under stirring. When the pH arrived 6, the formed precipitate was filtrated and then dried at 105 °C for 12 h. The morphologies of the samples are shown in Figure 2.1. The sample synthesized using zinc chloride aqueous solution is some broken hollow particles, while the sample synthesized using zinc sulfate aqueous solution is irregular particles. The reason is the effect of anions, of which Cl anions are beneficial to the formation of tubular particles.

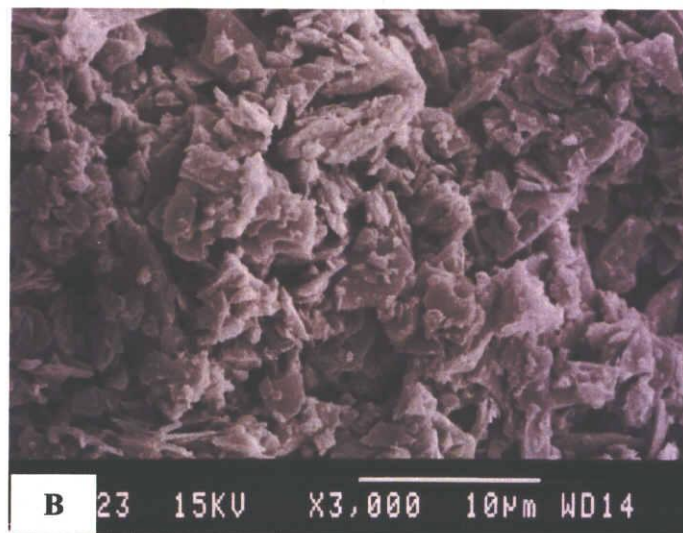


Figure 2.1 SEM images of samples (A-using zinc chloride aqueous solution, B-using zinc sulfate aqueous solution)

2.3 Experimental procedure

2.3.1 Starting materials

All of the reagents were of analytical grade and were used as received. Zinc chloride of at least 98 % purity and ammonia water of 25 % concentration (From Wako pure chemical industries, Ltd. Japan), were used as received without further purification. Reaction solution of zinc chloride was prepared by the dissolution of the appropriate amount in distilled water.

2.3.2 Synthesis method

Figure 2.2 and Figure 2.3 are flowchart and schematic diagram of synthesis procedure for fabricating ZnO microtubes by the introduction of ammonia bubbles, separately. The conical flask with the aqueous solution (400ml) of Zinc Chloride (purity of 98% from Wako, Osaka Japan), of which Zinc ionic concentration is 0.5M, was put into a water bath, which control the suitable temperature of synthesis system (90 °C). The solution was stirred at the constant rate by the Teflon-coated magnetic stirring bar. The ammonia bubbles were introduced into the bottom of the solution through a micro-sized bubble maker (Tekeno, Japan) until a suitable pH value was reached. The precipitate was obtained as soon as the ammonia bubbles were added into the reaction solution. When the pH value of the reaction solution reached given pH, the ammonia bubbles was immediately stopped. The white precipitate was filtered, and then the

as-prepared samples were dried at 90 °C for 24 h.

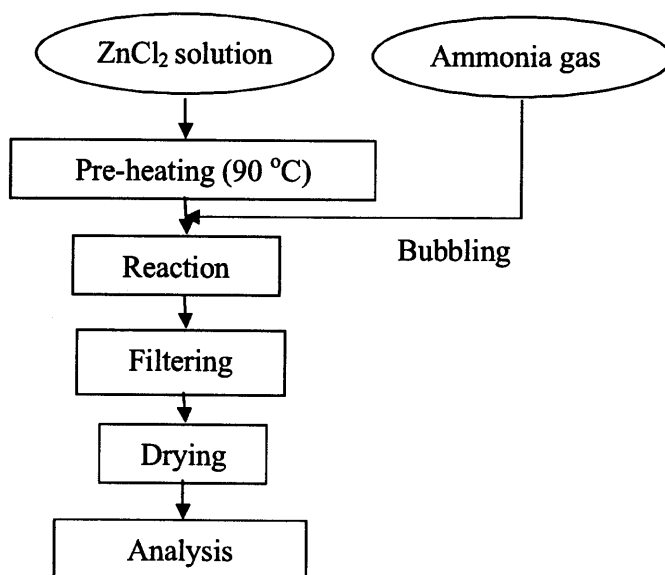


Figure 2.2 Flowchart of synthesis procedure for fabricating ZnO microtubes by the introduction of ammonia bubbles

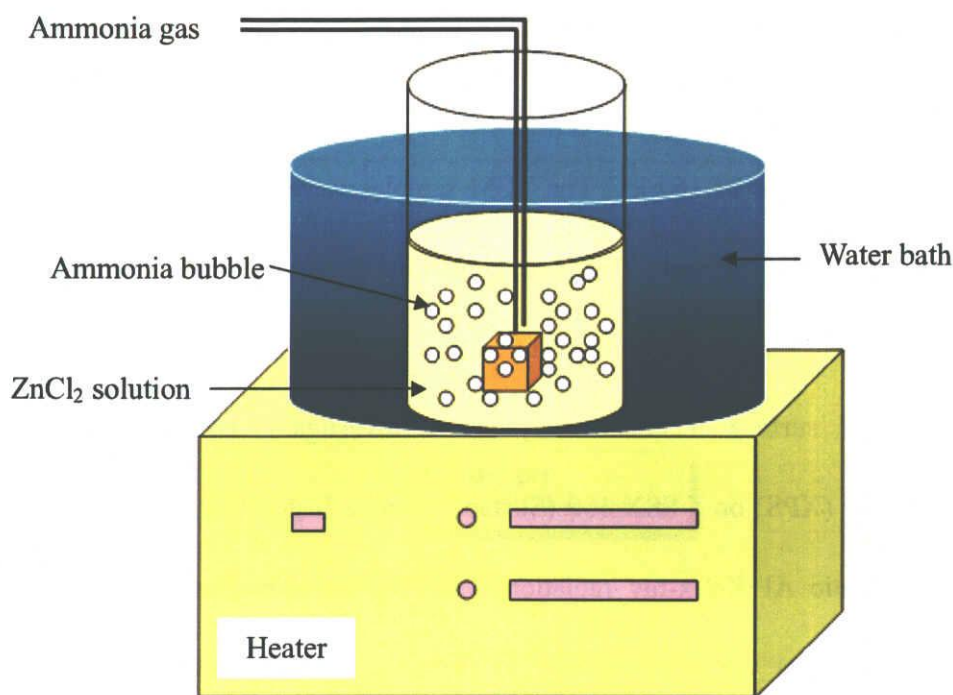


Figure 2.3 The schematic diagram of preparation procedure for fabricating ZnO microtubes by the introduction of ammonia bubbles

2.3.3 Characterization

The crystallographic structures of as-synthesized samples were characterized by X-ray diffraction (XRD, RINT1100, Rigaku, Japan) by employing a scanning rate of 0.02°/s in the 2θ range from 3 ° to 90 ° with $\text{CuK}\alpha_1$ (40 kV, 30 mA) radiation. The content of elements was examined by the energy dispersive X-ray spectroscopy (EDS).

The morphologies of products were examined by field emission scanning electron microscope (SEM, JSM-7000F, JEOL, Japan). Transmission electron microscopy was performed using the JEM2000 EXII TEM equipment (JEOL, Japan) with an accelerating voltage of 160 kV. The TEM samples were prepared by embedding the precipitates in polymer resin, followed by cutting the samples into a thickness of 200 nm. The cutting sample was carried out using a LEICA EM U6 ultramicrotome (Leica, U.S.A.). The surface chemical analysis was investigated by X-ray photoelectron spectroscopy (XPS) on a SSX-100 (Surface Science Instrument, USA) instrument. A monochromatic Al $K\alpha$ x-ray radiation was used as excitation source in the XPS measurement. For the determination of the unknown layer-like particles, TG/DTA analysis (Thermo Plus TG 8120, Rigaku, Japan) was carried out in nitrogen atmosphere. The heating rate was at 10 °C/min until 900 °C with 250 ml/min flow rate of nitrogen.

2.4 Effect of the pH on the formation of ZnO microtubes

Figure 2.4 shows the change of pH and temperature during reaction. The starting pH was about 4.5. After the introduction of ammonia bubbles into solution, the pH started to increase, while the temperature of solution sharply increased firstly and then decreased, which indicated that it was an exothermic reaction for the formation of zinc oxide. The increase of temperature was slowed down, when the reaction was nearly

ending.

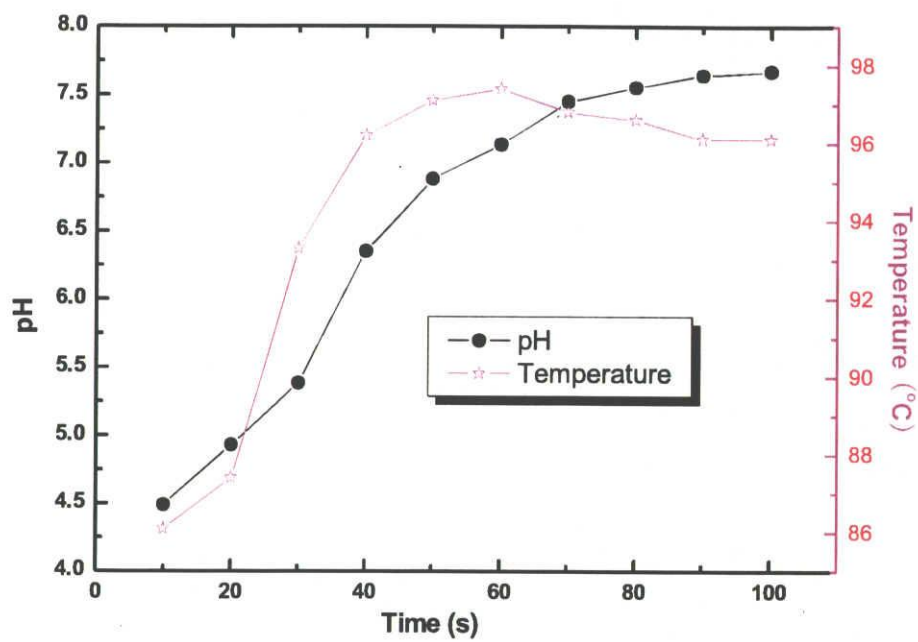


Figure 2.4 Dependence of pH and reaction temperature on reaction time

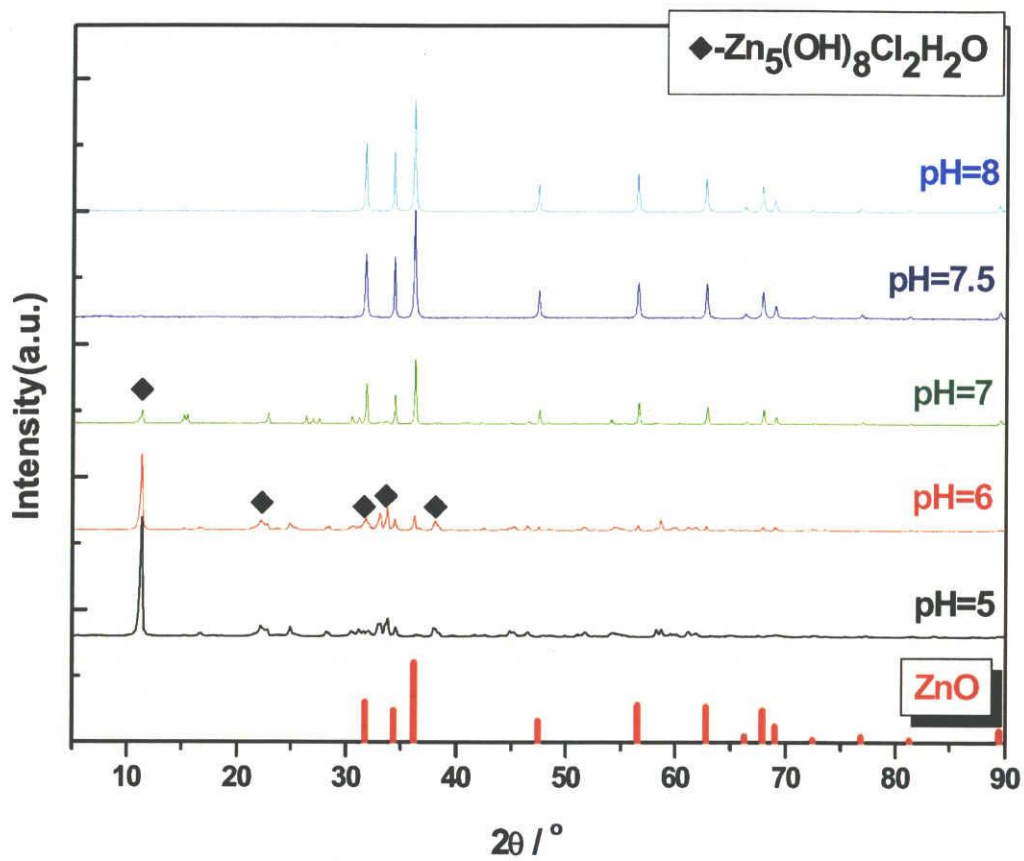
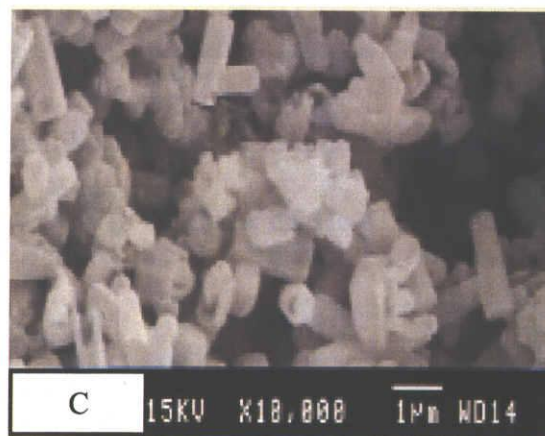
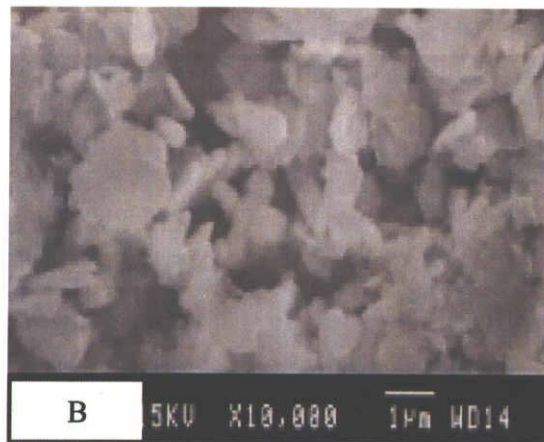
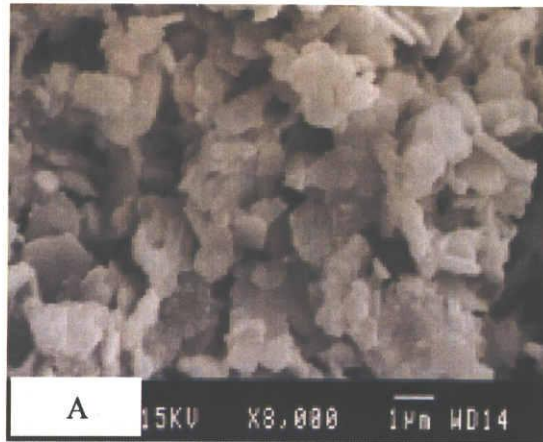


Figure 2.5 XRD patterns of the products prepared at different final pH

Figure 2.5 shows the XRD patterns of the samples prepared at different final pH. It was found the products were mostly zinc hydroxide chloride precursor ($\text{Zn}_5(\text{OH})_8\text{Cl}_2\text{H}_2\text{O}$), when the pH was 5 or 6. However, when the pH was over 7.5, the products became pure zinc oxide, which peaks can be indexed to the hexagonal phase of zinc oxide (wurtzite structure, space group P63mc). The lattice parameters were calculated to be $a=3.25$, $c=5.21$, which agreed well with the reported value (JCPDS card NO 36-1451) and there was no characteristic peaks of impurities observed, such as $\text{Zn}(\text{OH})_2$, zinc hydroxide chloride precursor. Therefore, it can be concluded that the formation of single crystalline was strongly dependent on the final pH of reaction solution in our experiments. Only at a relative high pH was it possible for the formation of the single crystalline ZnO.

The pH conditions must have great influence on the morphologies and the phase stability of precipitate. The addition of ammonia bubbles can increase the amount of the precipitates. Figure 2.6 shows the SEM images of the samples prepared at different final pH. Figure 2.6 (A) and Figure 2.6 (B) are the images of samples prepared at pH 5 and 6, respectively. The products were layer-like irregular particles without the observation of zinc oxide tubes. However, many incomplete zinc oxide tubes were observed in Figure 2.6 (C) at pH 7. The average diameter of the tubes was in the 300nm~500nm with the length in the 1 μm ~2 μm and the thickness of the wall was in the 20nm~50nm. When the pH is over 7.5, almost all products were tube-like or rod-like particles, as shown in Figure 2.6 (D) and Figure 2.6 (E). These results are expected since Zn ions are quite

sensitive to the pH conditions. It is reported that Zn ions exist in different forms in the aqueous solution with different pH conditions, that is, $ZnCl_n(OH)_{6-n}$ in acid or neutral conditions [13] , $Zn(OH)_4^{2-}$ in basic solution [14] and $Zn(OH)_4^{2-}$ and $Zn(NH_3)_4^{2+}$ in alkaline ammonia aqueous conditions [15, 16]. Accordingly, the growth units are different, which is supposed to affect the growth rate of the crystalline facets and final morphologies of the product.



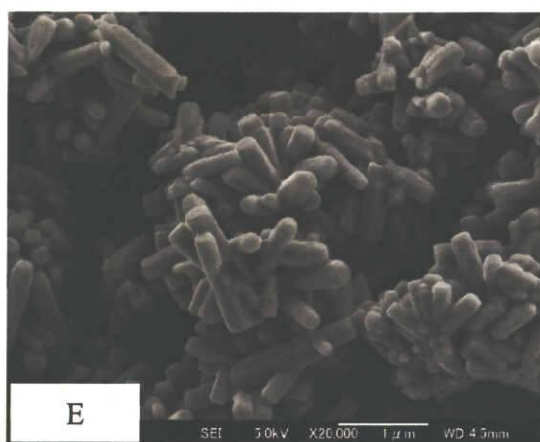
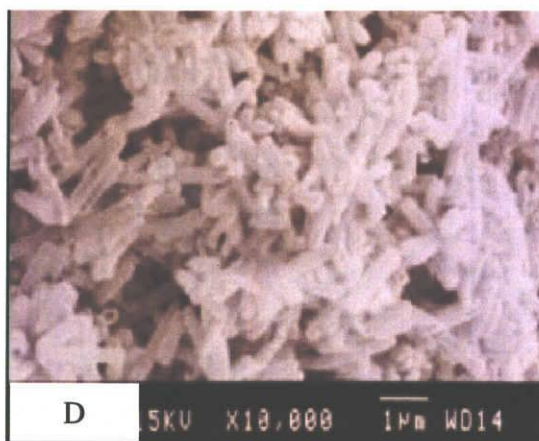


Figure 2.6 SEM images of samples prepared at different final pH
(A-pH 5, B-pH 6, C-pH 7, D-pH 7.5 and E-pH 8)

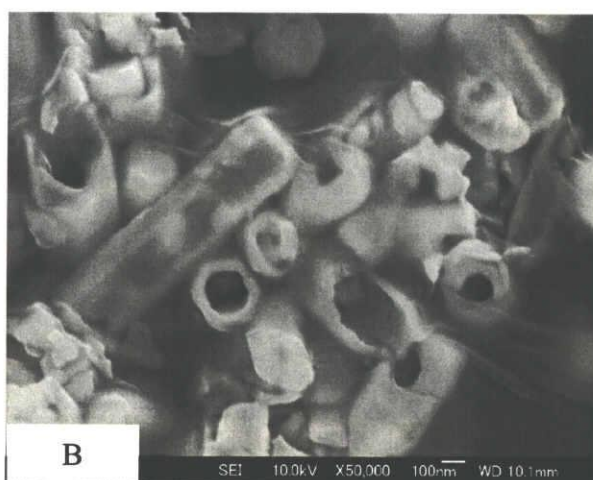


Figure 2.7 SEM images of cutting surface of the rod-like particles (pH=8)

Figure 2.7 is the morphology of the cutting surface of the rod-like zinc oxide particle when pH is nearly 8. The cuttings of samples were carried out by putting samples into the polymer, and then dried at 60 °C for 12 hours to solidify polymer. The cutting slices were carried out by LEICA EM UC6. From Figure 2.7, it is found that almost all rod-like particles have hollow structure inside.

2.5 Optimization of drying conditions

2.5.1 Open heating system and close heating system

In order to investigate the effect of H₂O on the formation of ZnO microtubes during the growth process, the precipitates were divided into two same holders. One holder without cover, which is called open heating system, and another with cover, which is called close heating system, were dried at constant temperature of 90 °C for 2 days in a regular laboratory oven, as shown in Figure 2.8 (A) and (B). Figure 2.8 (a) and (b) are the schemes of open heating system and close heating system, separately. The precipitate was dried at open heating system, which results in quickly evaporating the water and increasing the concentration of the ions and growth units. While the precipitate was dried at close heating system, which developed the water circulation due to the slow evaporation.

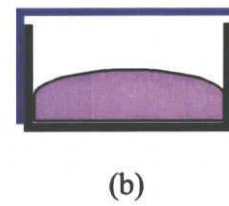
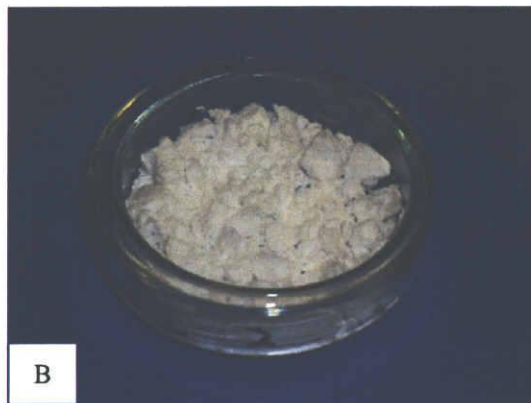
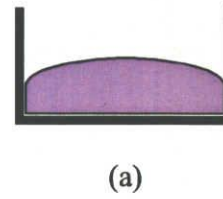


Figure 2.8 Photographs of open heating system and close heating system before dried at 90 °C (A- open heating system; a- scheme of open heating system; B- close heating system; b-scheme of close heating system)

Table 2.1 The weight of samples before and after drying at close heating system and open heating system

	Weight of sample dried at close heating system (g)	Weight of sample dried at open heating system (g)
Before drying	16.594	16.615
After drying	5.021	6.126
Weight loss (%)	69.7	63.1

The weight of sample before and after drying at close heating system and open heating system is shown in Table 2.1. The weight loss of sample dried at close heating system is higher than that dried at open heating system.

Figure 2.9 is the corresponding XRD pattern and SEM image of the samples dried at open heating system. From XRD result, almost all peaks can be indexed as the hexagonal phase of ZnO, which is not well crystalline. And the product still contains the precursor. SEM image shows the irregular structure rather than ZnO microtubes or microrods. The purity and crystallographic and morphology of the samples dried at the close heating system were examined using XRD and SEM, as shown in Figure 2.10. The sharp shape of the diffraction peaks suggests that the synthesized ZnO samples should be well crystallized and can be indexed to the hexagonal phase of zinc oxide (wurtzite structure, space group P63mc). And there were no characteristic peaks of

impurities observed. From SEM images, the morphology of product is rod-like and tube-like particles.

During the process of synthesizing ZnO microtubes via the aqueous solution, heterogeneous nucleation competes with the homogeneous one. The mechanism of heterogeneous nucleation is the adsorption process of growth unit $Zn-O_x(OH)_y$ complex, which occurs in the solid-liquid interface. The homogeneous nucleation is the direct deposition of atom clusters in the solution. In the close heating system, Thus, H_2O has an effect on the nucleation process markedly. The irregular ZnO layer-like particles synthesized under the open heating system are attributed to the homogeneous nucleation. On the contrary, under the close heating system, the heterogeneous nucleation coexists with the homogeneous nucleation due to the circled water. The growth units encapsulated the water are adsorbed to the particles through the homogeneous nucleation, which is the process of heterogeneous nucleation.

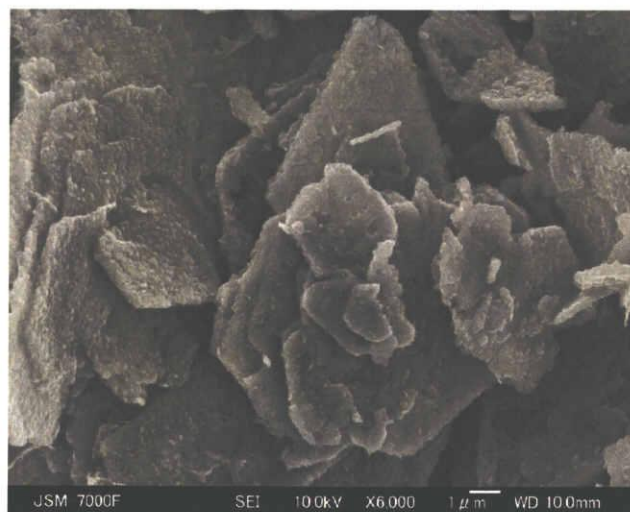
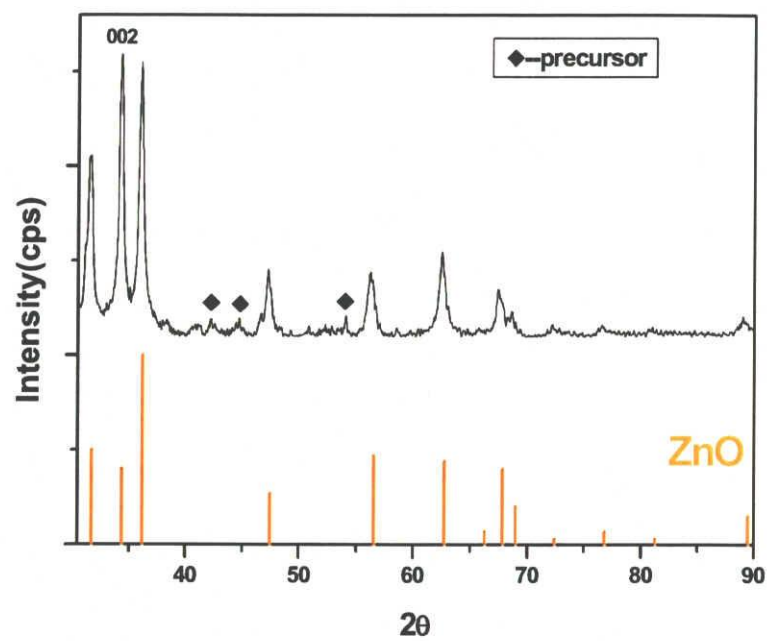


Figure 2.9 XRD pattern and SEM image of samples dried at open heating system at 90 °C for 2 days

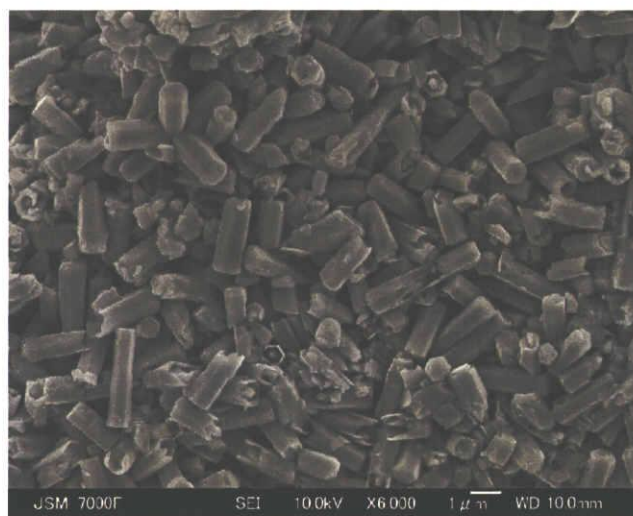
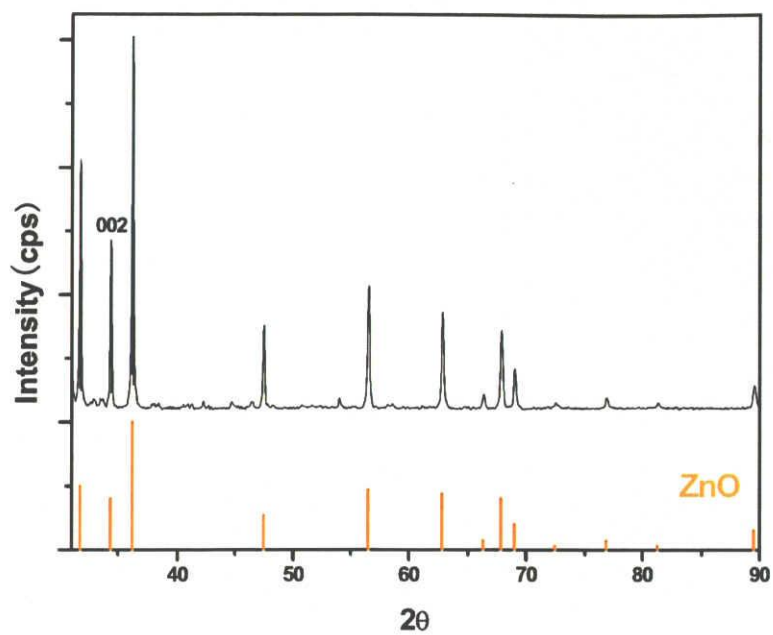


Figure 2.10 XRD pattern and SEM image of samples dried at close heating system at 90 °C for 2 days

2.5.2 Effect of drying temperature

To investigate the growth mechanism of ZnO microtubes by a soft aqueous solution synthesis, a series of controlled experiments were carried out with changing drying temperature during the heat treatment.

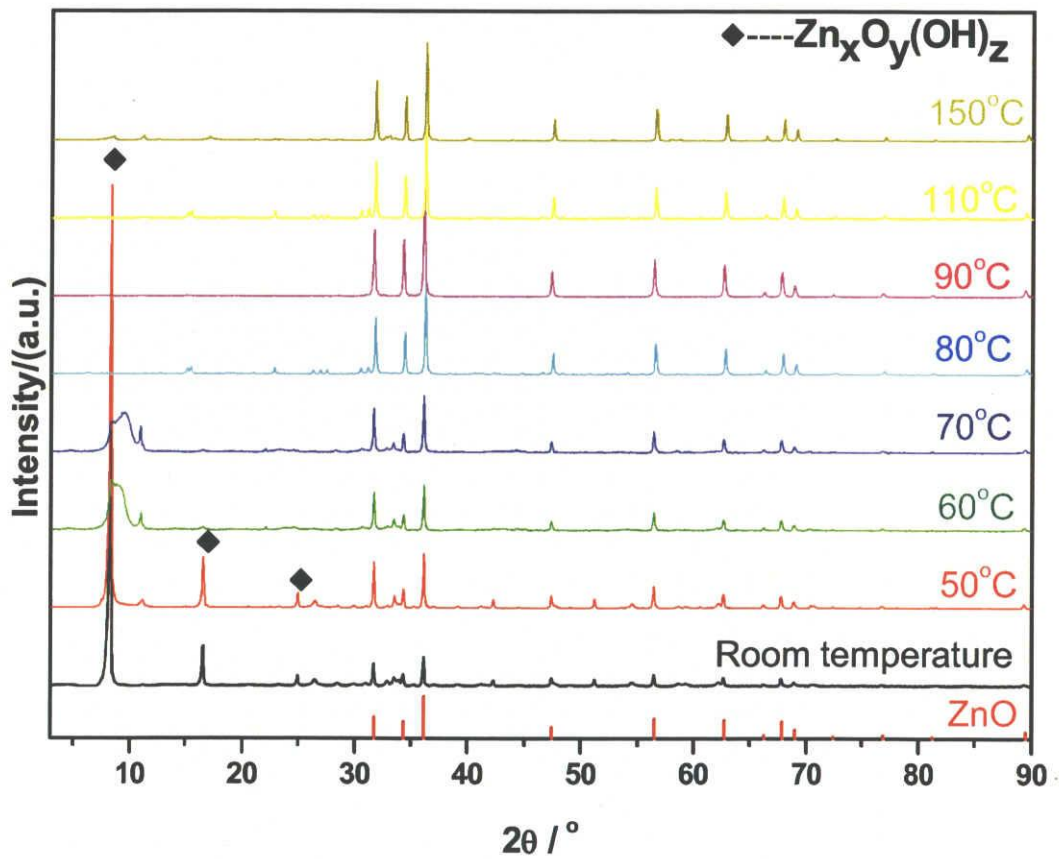
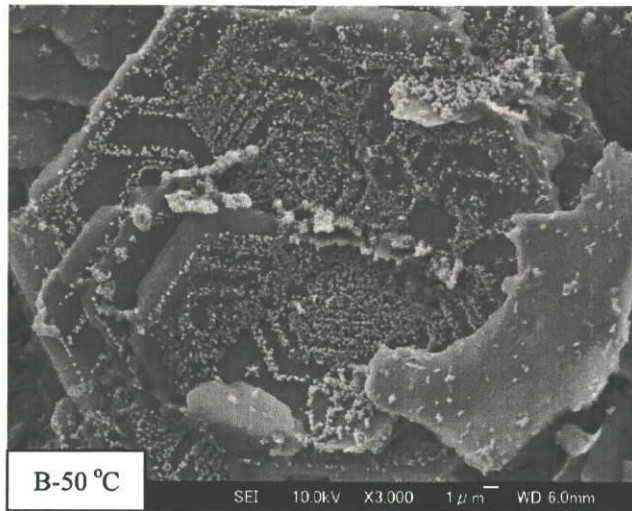
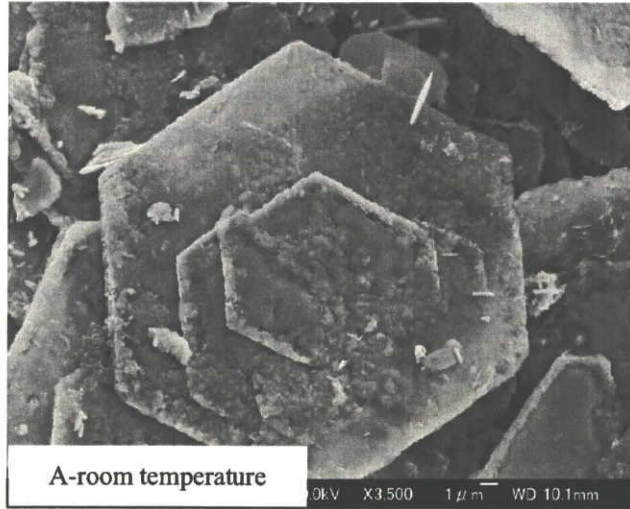
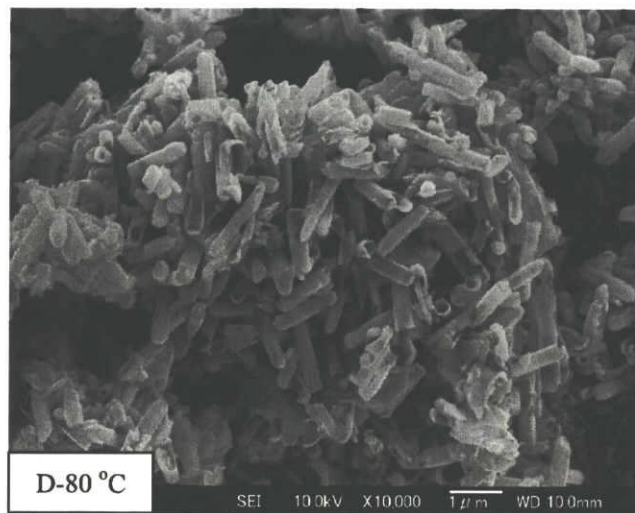
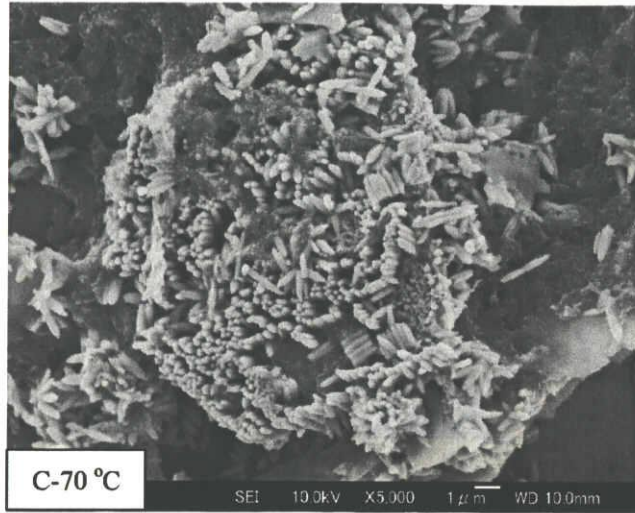


Figure 2.11 XRD patterns of the products prepared at different drying temperature

Figure 2.11 shows the XRD patterns of the products prepared at different drying temperature. The products were mostly a kind of unknown materials, which can not be indexed in the database of XRD, when dried at room temperature. That material may be the hydrate of zinc. With the drying temperature increase, the unknown material is decomposed and the characteristic peaks of ZnO are appeared. While the drying temperature was over about 80 °C, the products were crystallized zinc oxide, and all peaks matched well with the hexagonal structure of zinc oxide (JCPDS No.36-1451). No characteristic peaks of impurities were observed. With the further increase of drying temperature, zinc oxide peaks sharpen and increase intensity, indicating that the formation of crystalline zinc oxide can obtain at higher temperature.





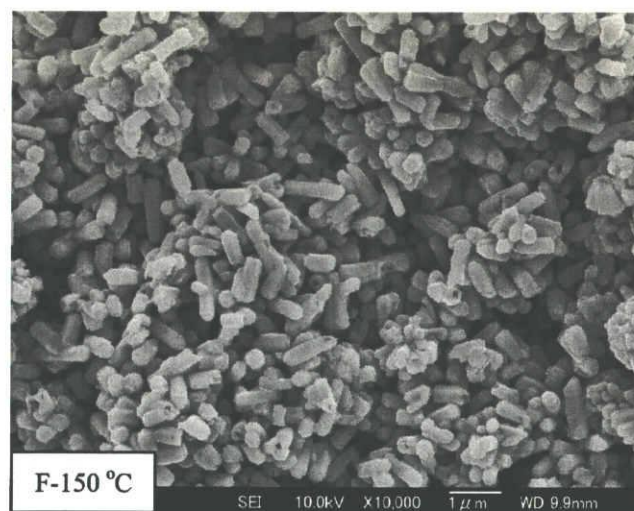
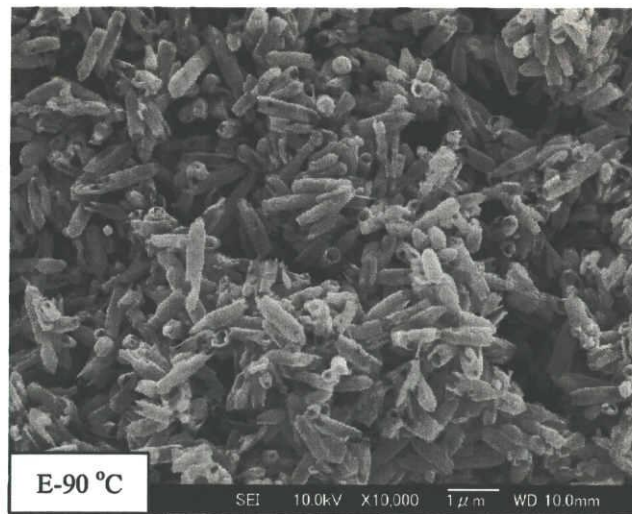


Figure 2.12 SEM images of the products prepared at different drying temperature (A-room temperature, B-50 °C, C-70 °C, D-80 °C, E-90 °C, F-150 °C)

Their shapes and morphologies at the drying process were investigated by SEM images. The morphology in the initial stage of precipitate is given in Figure 2.12 (A). It can be clearly seen that the particles were in the form of the regular hexagonal layer-like structure. The length of the hexagonal side was about 5~10 μm . After being dried at 50 $^{\circ}\text{C}$ for 12 h, as shown in Figure 2.12 (B), layer-like particles begin to decompose into crystal grains. Figure 2.12 (C) clearly reveals that ZnO rod-like growing at 70 $^{\circ}\text{C}$: some of particles still kept the layer-like, while others already have the rod-like particles with the length of more than 500 nm. Figure 2.12 (D) - Figure 2.12 (F) show the SEM images of the samples obtained when dried at 80 $^{\circ}\text{C}$, 90 $^{\circ}\text{C}$ and 150 $^{\circ}\text{C}$. From SEM images, the sample dried at over 80 $^{\circ}\text{C}$, ZnO microtubes grow both in size and morphology. And ZnO microtubes have the length of about 1 μm . The best drying temperature is 90 $^{\circ}\text{C}$. The above experiments and results manifested that the drying temperature plays an important role on the formation of ZnO microtubes.

2.6 Liquid nitrogen frozen system

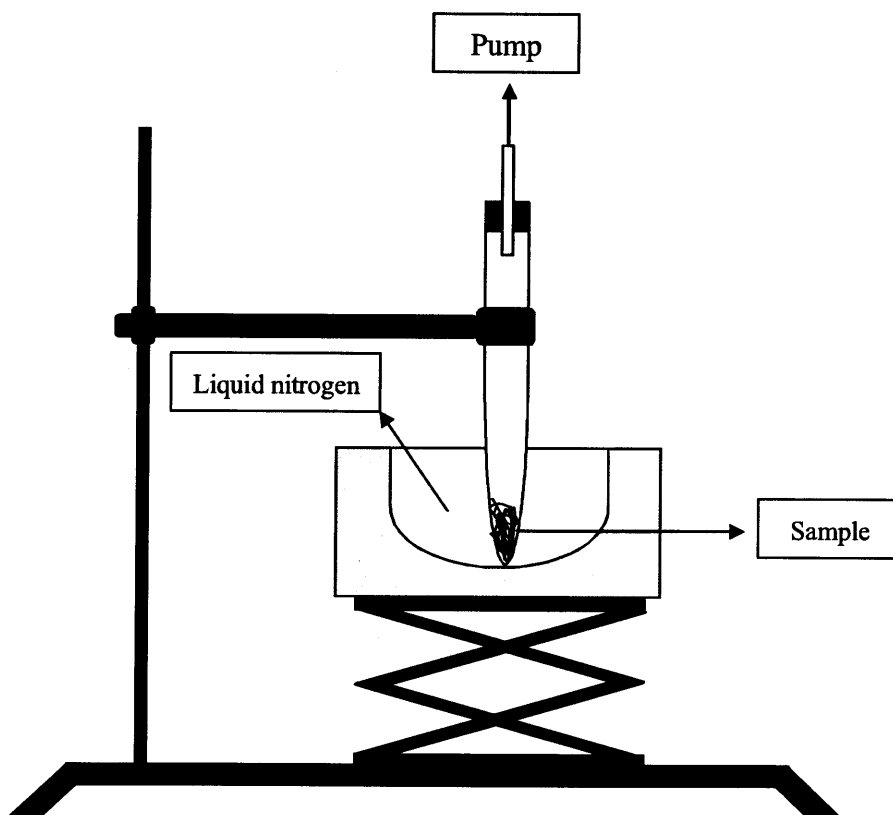


Figure 2.13 Setup of liquid nitrogen drying system

The aim of this experiment, which the precipitate is dried at liquid nitrogen system to keep it react and decompose, is to investigate the morphology and compositions of the product directly precipitated in the solution with and without aging duration. Whether the morphology and composition of sample dried at room

temperature is as same as the precipitate directly in the solution. The setup of liquid nitrogen drying system is shown in Figure 2.13. The sample was put in a glass tubes kept in the liquid nitrogen. During the drying process, steady flow pumping is carried out for 4 h to keep the low vacuum until the sample dried.

From Figure 2.14 SEM images of samples dried at room temperature in air and Figure 2.15 SEM images of samples dried at liquid nitrogen drying system, both of their morphologies are hexagonal layer-like with 5-10 μm layer-size without aging duration and hexagonal rod-like particles with aging duration for 24 h. The compositions of dried samples are investigated using XRD, as shown in Figure 2.16. Not only the sample dried at the room temperature in air but also dried in liquid nitrogen drying system is the sharp characteristic peaks of unknown material without aging duration, as shown in Figure 2.16 (A). While the aging time is 24 h, both of them are mostly crystalline zinc oxide particles; however still contain some precursors as shown in Figure 2.16 (B).

The morphology of precipitate, which is directly filtrated from the reaction solution after the introduction of ammonia bubbles when pH is 7.5, is layer-like. That is to say, the formation of ZnO microtubes is in the drying process, which was excluded from the formation mechanism of ZnO microtubes using ammonia bubbles as template.

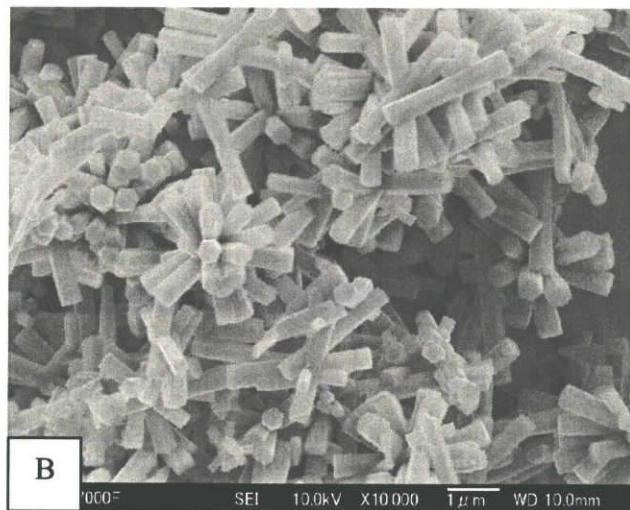
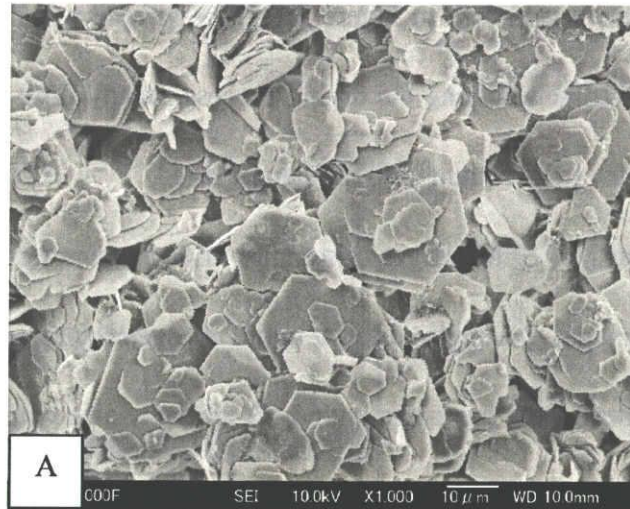


Figure 2.14 SEM images of the samples dries at room temperature in air (A-aging time= 0 h; B-aging time= 24 h)

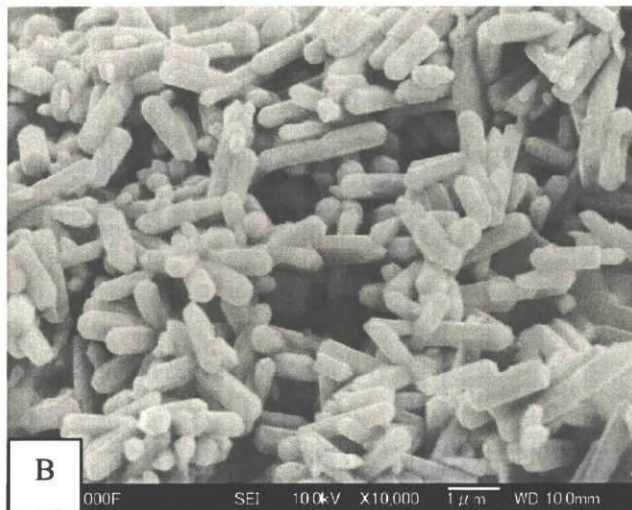


Figure 2.15 SEM images of the samples dried in liquid nitrogen drying system (A-aging time= 0 h; B-aging time= 24 h)

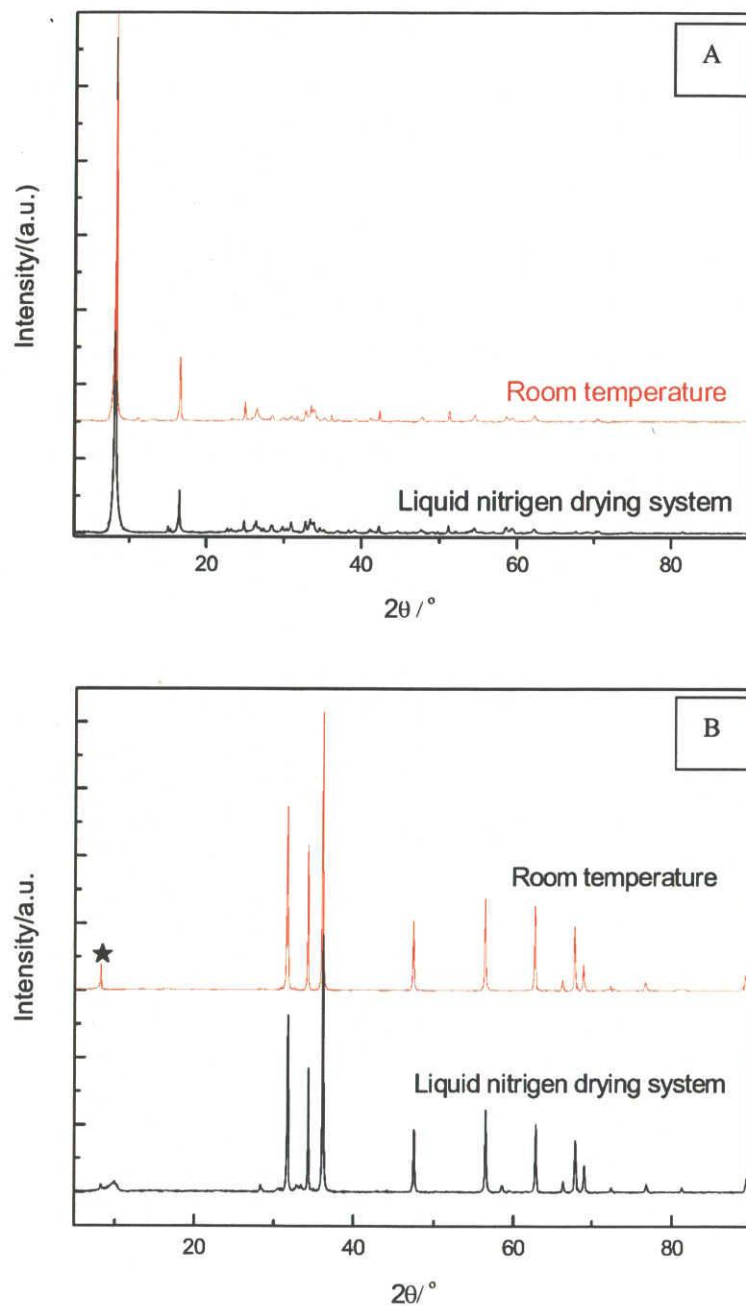


Figure 2.16 XRD patterns of the samples dried at room temperature in air and in liquid nitrogen drying system (A-without aging; B-with aging for 24 h)

2.7 Analysis of the particles dried at room temperature

In the previous work, the hexagonal layer-like unknown structure, which is prepared at pH 7.5, may be the compound of zinc and oxygen.

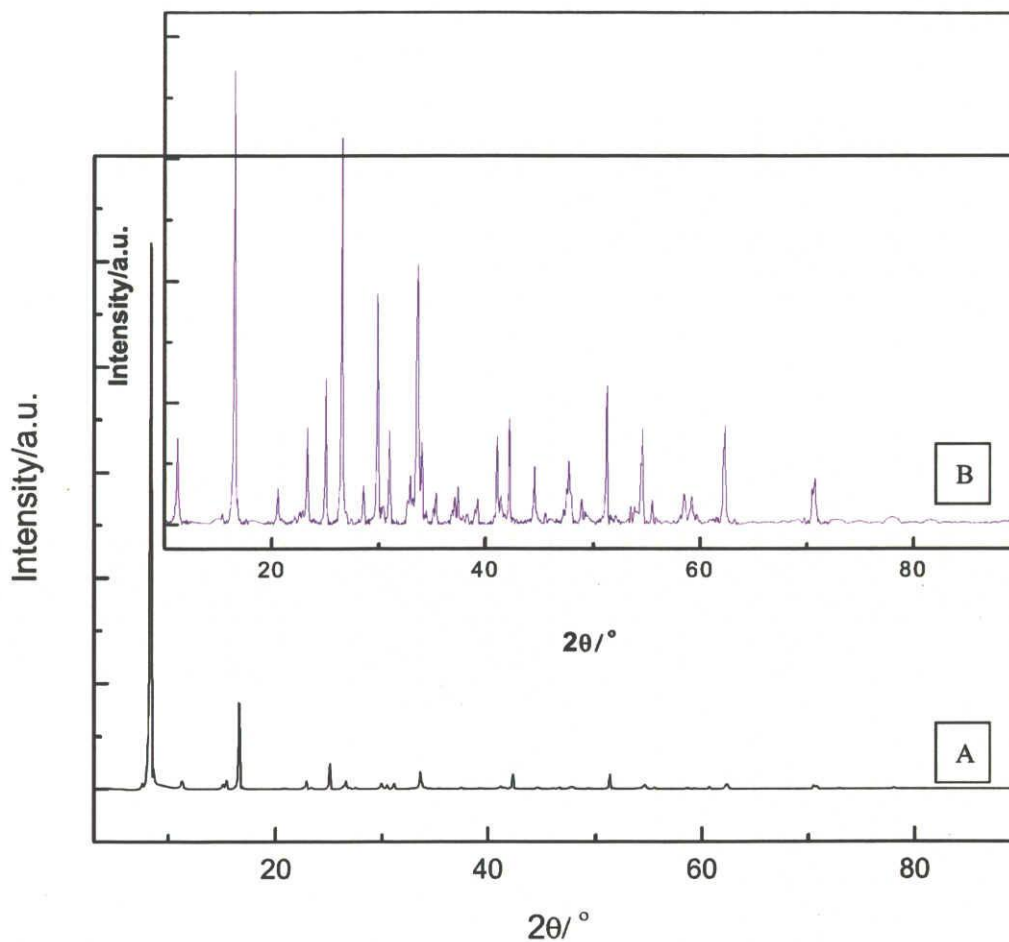


Figure 2.17 XRD patterns of the unknown layer-like particles

(A-from 3 ° to 90 °; B- from 10 ° to 90 °)

Figure 2.17 shows XRD patterns of the unknown layer-like particles. Figure 2.17 (A) is the range from 3° to 90° , there is a highest peaks located at 8.2° . In order to clearly obtain other peaks, the range from 10° to 90° is investigated. Besides the highest peaks, there still exist other peaks, which also can not be indexed in JCPDS card. It indicates that the precursor maybe contain several kinds of hydrate of zinc oxide.

To investigate whether it contains other impurities, such as Cl^{-} , N^{3+} , and the products were analyzed using XRD, EDS, XPS and TG-DTA.

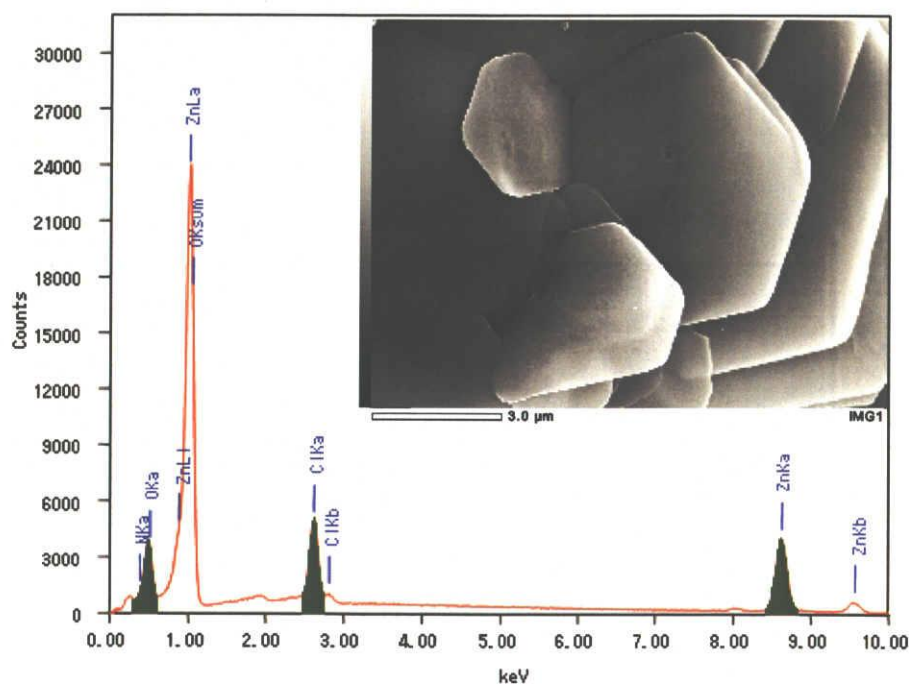


Figure 2.18 EDS analysis of the unknown layer-like particles

Table 2.2 EDS analysis result of the unknown layer-like particles

Element	Energy (kev)	Mass (%)	Atomicity (%)
N	0%	0%	0%
O	0.525	4.79	16.38
Cl	2.621	5.63	8.69
Zn	8.630	89.58	74.93

The results of EDS analysis is shown in Figure 2.18 and Table 2.2. From EDS results, the unknown samples are composed by Zn, O and Cl, of which the atomic percentage is 74.93%, 16.38%, 8.69%, separately. However, from XPS spectra of unknown layer-like particles, as shown in Figure 2.19, only exist two kind of atoms—zinc and oxygen. The reason caused the different results between EDS and XPS is the range of analysis area. The analysis area of EDS is larger than that of XPS. Cl⁻ ions were partly adhered to the surface of the sample.

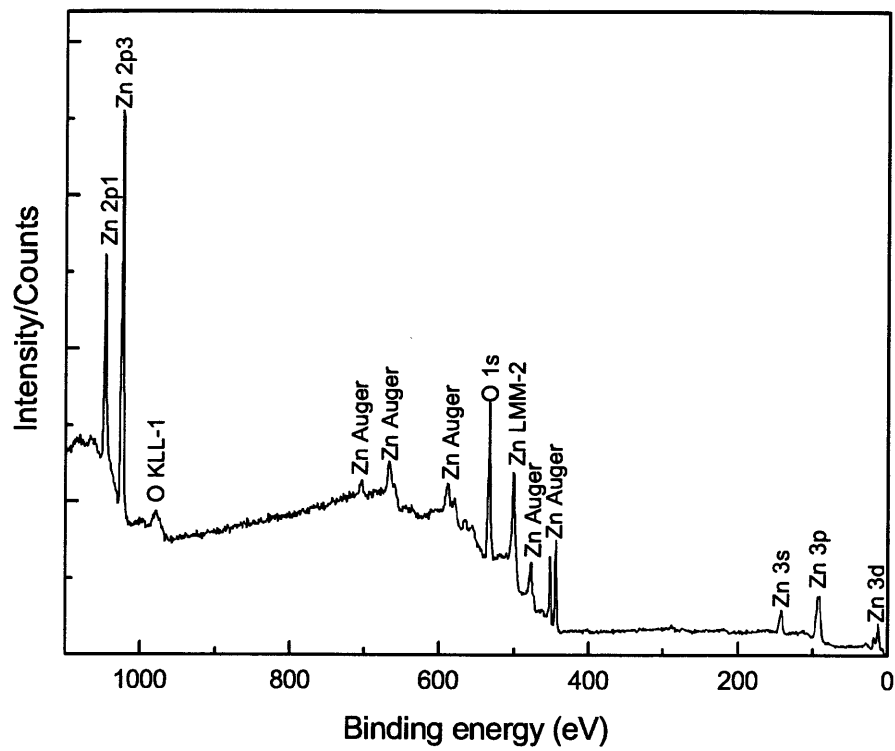


Figure 2.19 XPS spectra of unknown hexagonal layer-like particles

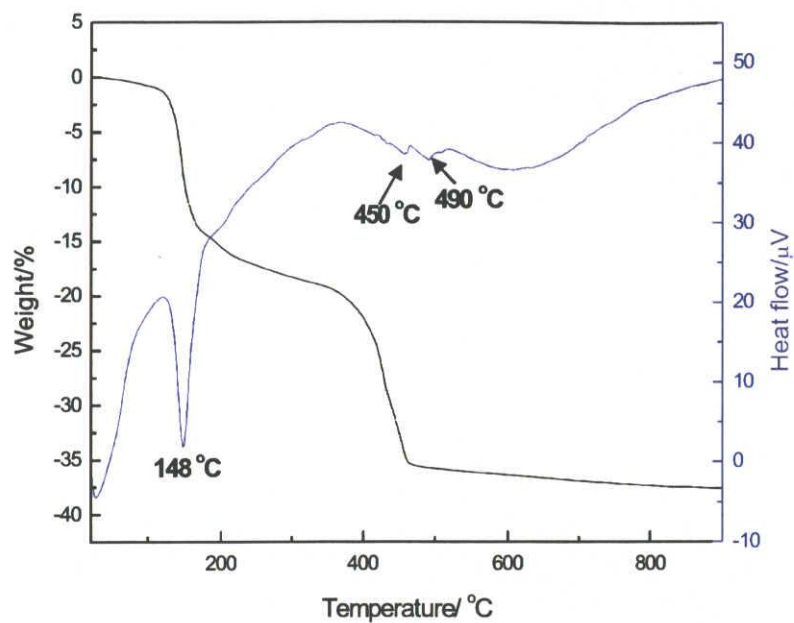


Figure 2.20 TG analysis of unknown hexagonal layer-like particles

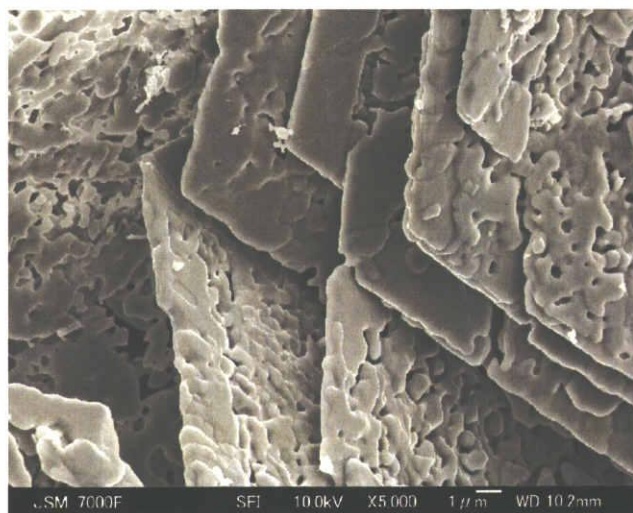


Figure 2.21 SEM images of unknown hexagonal layer-like particles after TG analysis

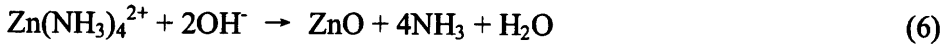
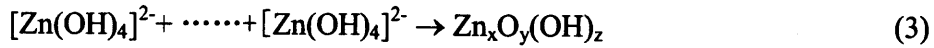
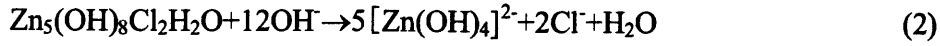
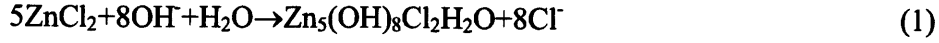
In order to further investigate the change of the unknown layer-like particles during the drying process, TG-DTA analysis was carried out. In the TG-DTA curve, as shown in Figure 2.20, there are three noticeable endothermic peaks at 148 °C, 450 °C, and 490 °C. The weight loss at 148 °C is about 13 %, which is attributed to the loss of crystalline water and the dehydroxylation process. The peaks located at 450 °C and 490 °C is attributed to the release of Cl⁻ and the oxygen, of which the weight loss is nearly about 15 %. After the TG analysis, the samples continue to perform XRD in order to investigate the morphological change. The layer-like particles with multiple-pole reticular structure is shown in Figure 2.21, which is attributed in the process of dehydration and dehydroxylation.

These series analysis confirm that the unknown products is the compound of $Zn_xO_y(OH)_z$, of which Cl⁻ ions are partly attached on the surface.

2.8 Reaction formula during the synthesis process

In the present case, rod-like and tube-like ZnO particles have been synthesized by the decomposition of the layer-like precipitate $Zn_xO_y(OH)_z$, to follow the growth habit of ZnO. This synthesis route gives suitable conditions and transitional intermediate of zinc hydroxide- $Zn_xO_y(OH)_z$ to obtain well-crystallized ZnO. Under the given pH and temperature, zinc is thought to exist primarily as $[Zn(OH)_4]^{2-}$ and $Zn(NH_3)_4^{2+}$. The $Zn_xO_y(OH)_z$ is formed by the decomposing of these intermediates.

Although the system is quite complex, the dominant chemical reaction processes can be expressed by the following formulas on the basis of our analysis and others [15-22].



After analysis of the above results and the dominant chemical reactions in the system, the growth process of the ZnO particles is more apparent. When the pH is 6, the precipitate is $\text{Zn}_5(\text{OH})_8\text{Cl}_2 \cdot \text{H}_2\text{O}$ precursor, which can't form the wurtzite ZnO particles. At a higher pH of reaction solution, which would be the key factor for controlling the composition of precursor, the formation of layer-like $\text{Zn}_x\text{O}_y(\text{OH})_z$ precursor via the solution route can be incorporate by decomposing $[\text{Zn}(\text{OH})_4]^{2-}$ and $\text{Zn}(\text{NH}_3)_4^{2+}$. $\text{Zn}_x\text{O}_y(\text{OH})_z$ is actually the precipitate filtrated immediately when the pH arrived 7.5. At the process of aging duration, rod-like ZnO with uniform size were achieved through dehydration of $\text{Zn}_x\text{O}_y(\text{OH})_z$ based on the anisotropy of ZnO special crystal structure. While the precipitate $\text{Zn}_x\text{O}_y(\text{OH})_z$ filtrated after the reaction was dried at 90 °C in air, the hexagonal ZnO microtubes can be obtained, since the dehydration in the coordination $\text{Zn}_x\text{O}_y(\text{OH})_z$ were removed faster and the liquid-gas and NH_4OH ionization equilibriums provide a crucial basic condition in the system. At the drying

system, the precipitate possesses higher crystal growth velocity, which is attributable to the high concentration of the growth units compared with in the reaction solution. At the growth process, the length of ZnO rods increases quickly, the morphology of ZnO will be directed to lower the system energy, directly transform to ZnO microtubes due to the higher energy at the ZnO polar surface.

2.9 Transmission Electron Microscopy analysis

Figure 2.22 shows the further characterization of the prepared tubes using TEM. Figure 2.22 (A) is the TEM images of a horizontally cut tube. The dark center and bright edge indicates the presence of hollow structure inside of the tube. The small particles observed inside of the tube are believed to be the result of cutting. The inset of Figure 2.22 (A) is an electron diffraction (ED) pattern selected from the wall of tube, which reveals that the tube was single crystalline.

The inset of Figure 2.22 (B) is an ED pattern selected from the hexagonal opening, which indicates that the tube is single crystalline and grew along [0001] direction (*c* axis). Regarding the ZnO crystal having a single crystallographic direction of [0001], it can be simply explained by the “lowest energy” argument, i.e., the hexagonal (0001) plane of ZnO with wurtzite structure is the closest packed plane in the crystal, and stacking along the [0001] direction, therefore, becomes energetically favorable. [23]

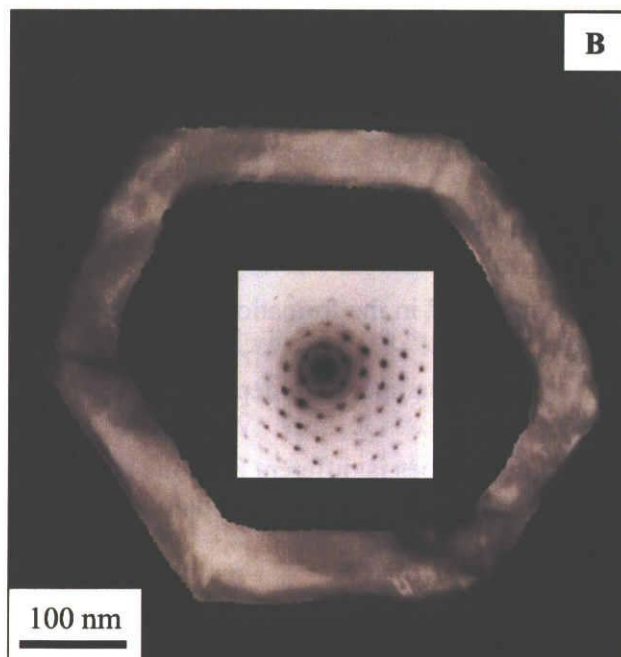
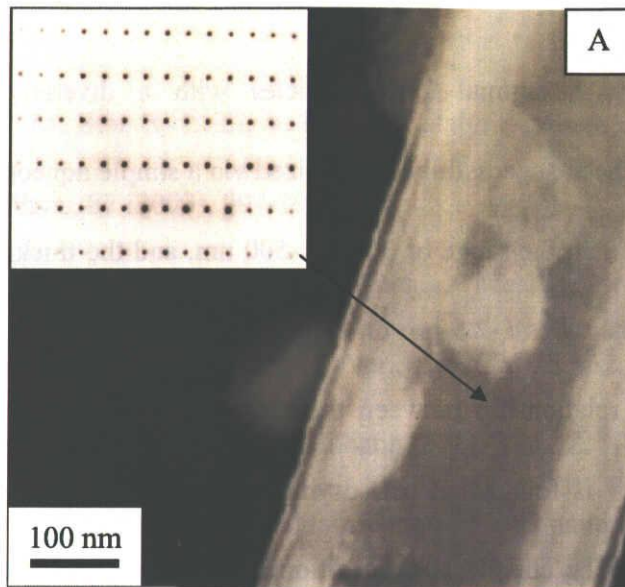


Figure 2.22 TEM images of ZnO microtubes synthesized and dried at 90 °C

2.10 Conclusion

In summary, hexagonal ZnO particles with a diversity of well-defined morphologies have been successfully synthesized via a simple aqueous route. The tubes presents the diameter in the range of 300 nm-500 nm, and the thickness of wall 30-50 nm, the length of the tubes 1-2.5 μm on average. To finely control the morphology of ZnO particles, the relationship between the morphology and the reaction conditions were investigated. It is found that pH, drying temperature have significant effect on ZnO morphologies. The chemical composition is mainly determined by the pH of the reaction solution. When the pH is 6, the obtained layer-like $\text{Zn}_5(\text{OH})_8\text{Cl}_2\cdot\text{H}_2\text{O}$ precursor can not form ZnO particles, of which the morphology is still layer-like when dried at higher temperature. While the pH is 7.5, the precipitate is layer-like $\text{Zn}_x\text{O}_y(\text{OH})_z$ that can form the wurtzite ZnO rods or tubes. The layer-like $\text{Zn}_x\text{O}_y(\text{OH})_z$ precursor dried at higher temperature can be attributed in the formation of ZnO microtubes.

And the series of drying temperature-dependent experiments reveal that the growth mechanism of ZnO microtubes is different from the bubble template method.

Reference

- [1] R. M. Wang, Y. J. Xing, Ju and D. P. Yu, "Fabrication and microstructure analysis on zinc oxide nanotubes", *New J. Phys.*, 5 (2003), 115.1-115.7.
- [2] Y. J. Xing, Z. H. Xi, Z. Q. Xue, X. D. Zhang, and J. H. Song, "Optical properties of

- the ZnO nanotubes synthesized via vapor phase growth”, *Appl. Phys. Lett.*, 83 [9] (2003), 1689-1691.
- [3] X. H. Kong, X. M. Sun, X. L. Li, Y. D. Li, “Catalytic growth of ZnO nanotubes”, *Mater. Chem. Phys.*, 82 (2003), 997-1001.
- [4] P. X. Gao, C. S. Lao, Y. Ding, and Z. L. Wang, “Metal/semiconductor core/shell nanodisks and nanotubes”, *Adv. Funct. Mater.*, 16 (2006), 53-62.
- [5] X. H. Zhang, S. Y. Xie, Z. Y. Jiang, X. Zhang, Z. Q. Tian, Z. X. Xie, R. B. Huang, and L. S. Zheng, “Rational design and fabrication of ZnO nanotubes from nanowire templates in microwave plasma system”, *J. Phys. Chem. B*, 107 [37] (2003), 10114-10118.
- [6] J. Zhang, L. D. Sun, C. S. Liao and C. H. Yan, “A simple route towards tubular ZnO”, *Chem. Commun.*, 2002, 262-263.
- [7] A. L. Yang, Z. L. Cui, “ZnO layer and tubular structures synthesized by a simple chemical solution route”, *Mater. Lett.*, 60 [19] (2006), 2403-2405.
- [8] B. Y. Geng, X. W. Liu, X. W. Wei, S. W. Wang, “Large-scale synthesis of single-crystalline ZnO nanotubes based on polymer-inducement”, *Mater. Res. Bull.*, 41 [10] (2006), 1979-1983.
- [9] J. X. Duan, X. T. Huang, E. K. Wang, “PEG-assisted synthesis of ZnO nanotubes”, *Mater. Lett.*, 60 (2006), 1918-1921.
- [10] Y. S. Han, G. Hadiko, M. Fuji, M. Takahashi, “Effect of Flow rate and CO₂ Content on the Phase and Morphology of CaCO₃ Prepared by Bubbling Method”, *J. Gryst.*

Growth, 276 (2005) 541-548.

- [11] G. Hadiko, Y. S. Han, M. Fuji, M. Takahashi, "Synthesis of Hollow Calcium Carbonate Particles by the Bubble Templating Method", *Mater. Lett.*, 59 (2005) 2519-2522.
- [12] Y. S. Han, G. Hadiko, M. Fuji, M. Takahashi, "A Novel Approach to Synthesize Hollow Calcium Carbonate Particles", *Chem. Lett.*, 34 (2005) 152-153.
- [13] D. J. Harris, Brodholt J. P., "Zinc Complexation in Hydrothermal Chloride Brines: Results from ab Initio Molecular", *J. Phys. Chem. A*, 107 (2003), 1050-1054.
- [14] L. N. Demianets, D. V. Kostomarov, I. P. Kuz'mina, S. V. Pushko, "Mechanism of Growth of ZnO Single Crystals from Hydrothermal Alkali Solutions", *Crystallogr. Rep.*, 47 (2002), S86.
- [15] J. Zhang, L. D. Sun, J. L. Yin, H. L. Su, C. S. Liao, and C. H. Yan, "Control of ZnO morphology via a simple solution route", *Chem. Mater.*, 14 (2002), 4172-4177.
- [16] S. Yamabi and H. Imai, "Growth conditions for wurtzite zinc oxide films in aqueous solutions", *J. Mater. Chem.*, 12 (2002), 3773-3778.
- [17] D. B. Wang, C. X. Song, Z. S. Hu, W. J. Chen, X. Fu, "Growth of ZnO prisms on self-source substrate", *Mater. Lett.*, 61 [1] (2007), 205-208.
- [18] S. Z. Li, S. M. Zhou, H. X. Liu, Y. Hang, C. T. Xia, J. Xu, S. L. Gu, R. Zhang, "Low-temperature hydrothermal growth of oriented [0001] ZnO film", *Mater. Lett.*, 61 [1] (2007), 30-33.

- [19] J. Jiang, G. C. Li, Q. M. Ji, H. R. Peng, "Morphological control of flower-like ZnO nanostructures", *Mater. Lett.*, 61 [10] (2007), 1964-1967.
- [20] A. W. Zhao, T. Luo, L. Y. Chen, Y. Liu, X. G. Li, Q. Tang, P. J. Cai, Y. T. Qian, "Synthesis of ordered ZnO nanorods film on zinc-coated Si substrate and their photoluminescence property", *Mater. Chem. Phys.*, 99 (2006), 50-53.
- [21] W. J. Li, E. W. Shi, W. Z. Zhong, Z. W. Yin, "Growth mechanism and growth habit of oxide crystals", *J. Gryst. Growth*, 203 (1999), 186-196.
- [22] Z. Wang, X. F. Qian, J. Yin, Z. K. Zhu, "Aqueous solution fabrication of large-scale arrayed obelisk-like zinc oxide nanorods with high efficiency", *J. Solid State Chem.*, 177 (2004), 2144-2149.
- [23] J. Q. Hu, Y. Bando, "Growth and optical properties of single-crystal tubular ZnO whiskers", *Appl. Phys. Lett.*, 82 (2003), 1401-1403.

**CHAPTER 3 SYNTHESIS OF ZnO NANO- AND MICRO-
TUBES USING AMMONIA WATER INSTEAD OF
AMMONIA BUBBLES**

3.1 Introduction

The formation mechanism of ZnO particles with tubular structure is not clear until now. There are few reports on synthesis mechanism of ZnO microtubes. And analyses of the microstructure and mechanism of ZnO microtubes are far from well understood. Anli Yang and Zuolin Cui [1] have reported that synthesis of ZnO tubular structure by scrolling of ZnO layer structure. Zhuo Wang et al. [2] have proposed that the growth mechanism of rod-like ZnO crystals formed from layered nanosheet particles stacking layer by layer and tubes particles obtained from the nanowires self-adjusting in a hexagonal circle and growing into tube-like particles. There explanations of mechanisms do not agree with the results of our work. That is because the thickness of layer is at least 300 nm, which is thicker than the wall thickness of ZnO tubes. Also the diameter of layer is much larger than one of rod-like particles.

In chapter 2, ZnO microtubes have been synthesized using the introduction of ammonia bubbles into the zinc chloride aqueous solution. The origin design is using ammonia bubbles as the soft template to prepare hollow ZnO particles. However, from Chapter 2, the morphology of the precipitate dried at room temperature is layer-like rather than tube-like. That means the formation mechanism of ZnO microtubes is different from the bubble template method.

In this chapter, in order to investigate the growth mechanism, improve and simplify the experimental process, synthesis of ZnO tubes is by using ammonia water

instead of ammonia bubbles. The effect of ammonia, reaction temperature and aging duration will be discussed. ZnO nanotubes will be synthesized through adjusting the concentration of zinc ions, reaction temperature and aging duration. The best percentage of ZnO microtubes and the yield of products will be shown.

3.2 Experimental procedure

3.2.1 Starting materials

All of the reagents were of analytical grade and were used as received. Zinc chloride of at least 98 % purity and ammonia water of 25 % concentration (From Wako pure chemical industries, Ltd. Japan), were used as received without further purification. The aqueous solution of zinc chloride was prepared by the dissolution of the appropriate zinc chloride in the distilled water.

3.2.2 Synthesis procedure

Figure 3.1 and Figure 3.2 are flowchart and schematic diagram of synthesis procedure for fabricating ZnO tubes by the introduction of ammonia water, separately. The conical flask with the aqueous solution (400 ml) of zinc chloride (purity of 98 % from Wako, Japan), of which zinc ionic concentration was 0.5 M, was heated in the oil bath under stirring. The synthesis temperature controlled by the oil bath was kept at

given temperature. Aqueous ammonia water (25%) was added dropwise into the reaction solution with stirring until a suitable pH value was 7.5. The precipitate was obtained as soon as the ammonia water was added into the reaction solution. When the pH value of the reaction solution reached 7.5, the ammonia water was immediately stopped. The white precipitate was aging at the reaction solution for given time and then filtered. Finally the as-prepared samples were dried at 90 °C for 24 h.

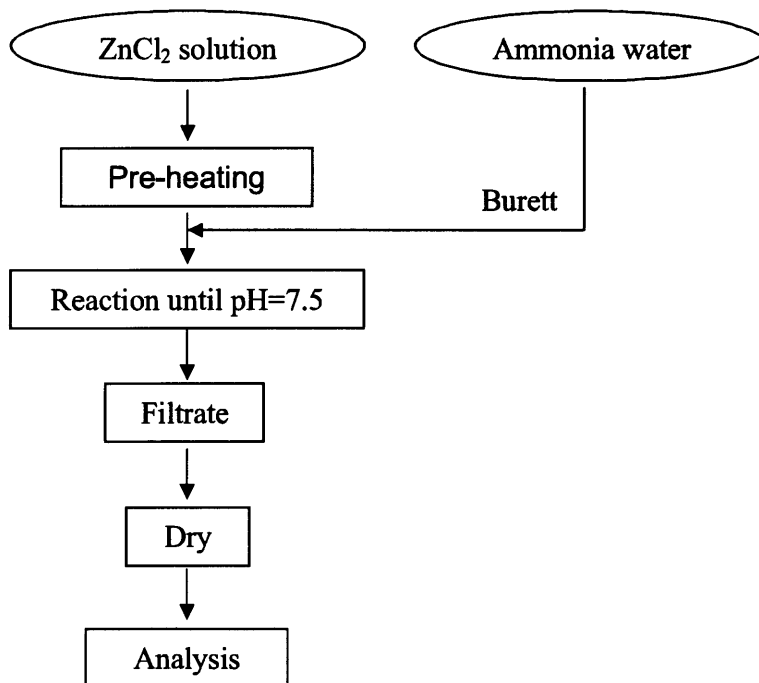


Figure 3.1 Flowchart for the formation of ZnO tubes using ammonia water

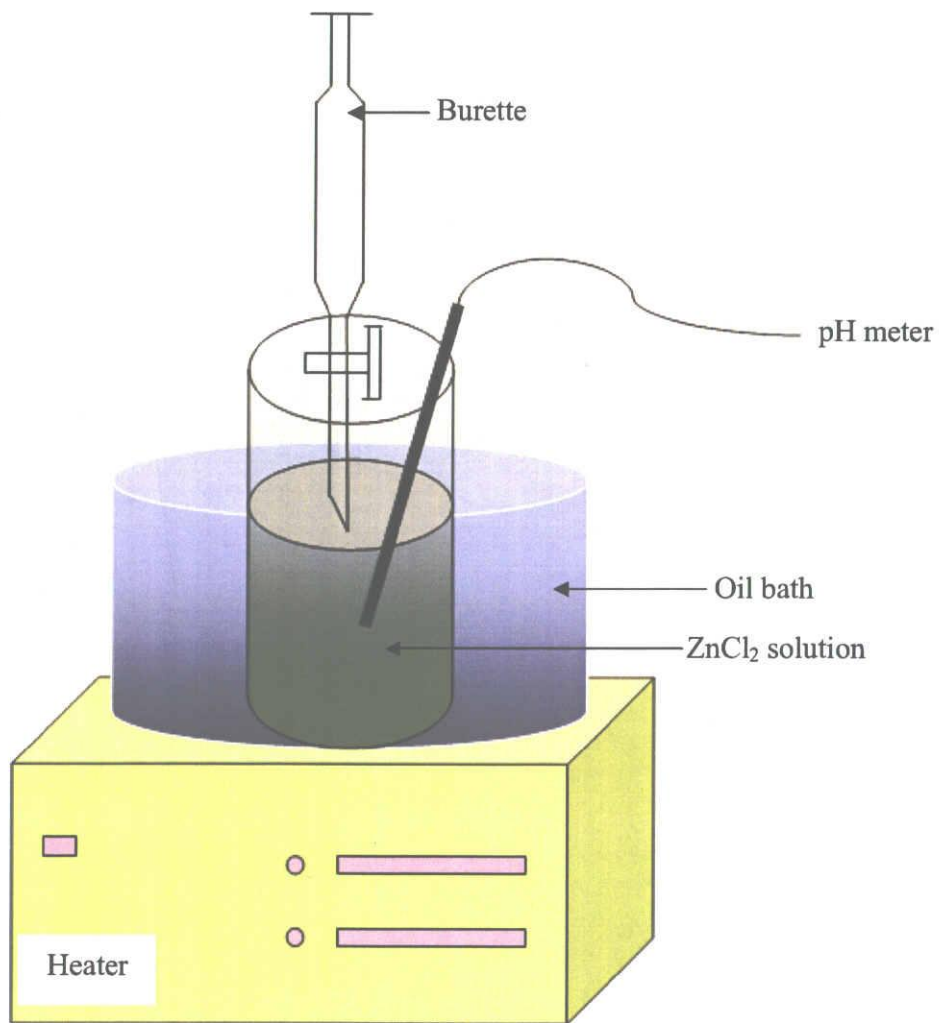


Figure 3.2 The schematic diagram of preparation procedure for fabricating ZnO tubes by the introduction of ammonia water

3.2.3 Characterization

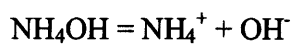
The compositions and crystallographic structures of as-synthesized samples were characterized by X-ray diffraction (XRD, RINT1100, Rigaku, Japan) by employing a scanning rate of 0.02°/s in the 2θ range from 3 ° to 90 ° with CuKα₁ (40 kV, 30 mA) radiation. The morphologies of products were examined by field emission scanning electron microscope (SEM, JSM-7000F, JEOL, Japan).

3.3 Effect of ammonia on the formation of ZnO microtubes

First, the effect of ammonia on the formation of ZnO microtubes is investigated in order to further propose a possible mechanism. The precipitates, which were prepared at pH 7.5, divided into two parts: one is directly dried at oven with the cover; the other is washed several times using the distilled water, and then dried as same as one.

Ammonia is thought to provide weakly basic conditions in the aqueous solution process when the precipitates are dried in atmospheric chemical oven. Although NH₄⁺ ions can coordinate with Zn²⁺ and form Zn(NH₃)₄²⁺, which is instable in a basic environment. When the temperature of reaction solution is maintained at 90 °C, as it would rapidly transform into ZnO. Figure 3.3 shows the SEM images of unwashed and washed sample using the distilled water. Comparison experiments show that ZnO microtubes only can be obtained when the unwashed precipitate dried at 90 °C. It was found that the washed sample led to the formation of irregular rod-like particles rather

than ZnO microtubes. It is worth that ammonia plays a crucial role, which is the key to construct tubular structure. It is known that ammonia can easily dissolved in water to give a basic environment, which ammonia can also be easily driven out of the precipitate during drying process. Then thus two equilibriums exist in the precipitate when it is heated in oven at 90 °C:



The liquid-gas and NH_4OH ionization equilibriums provide the weakly basic growth conditions in the drying system.

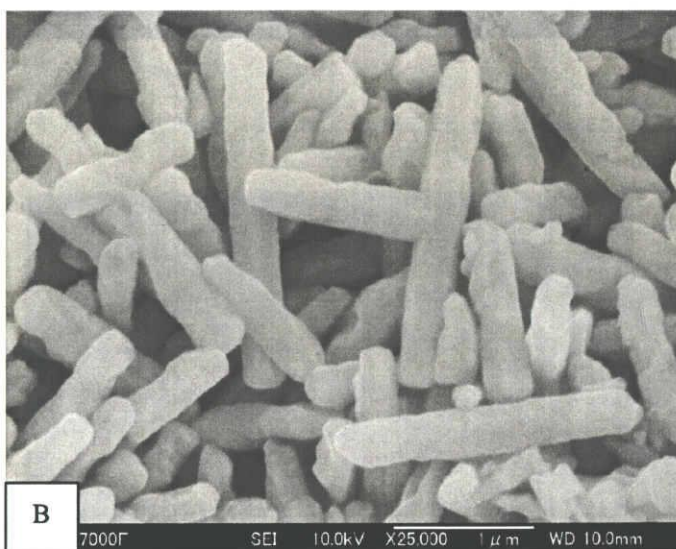
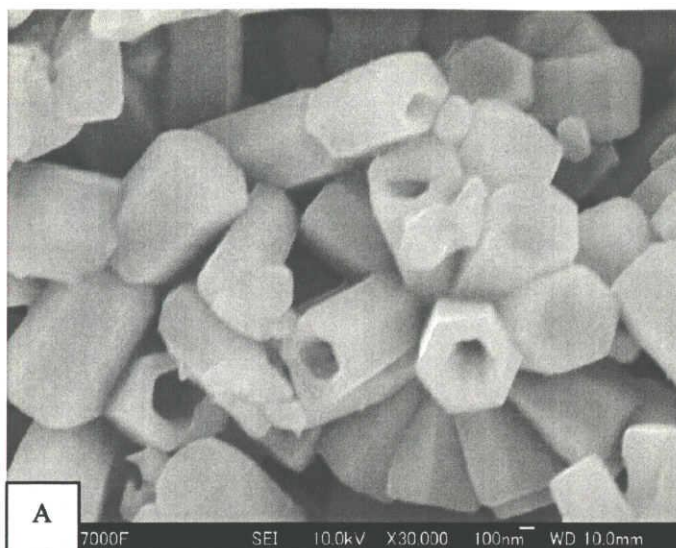
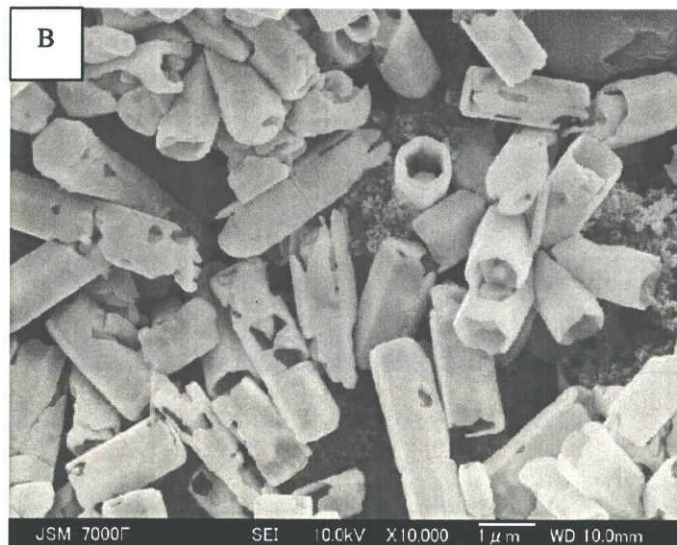
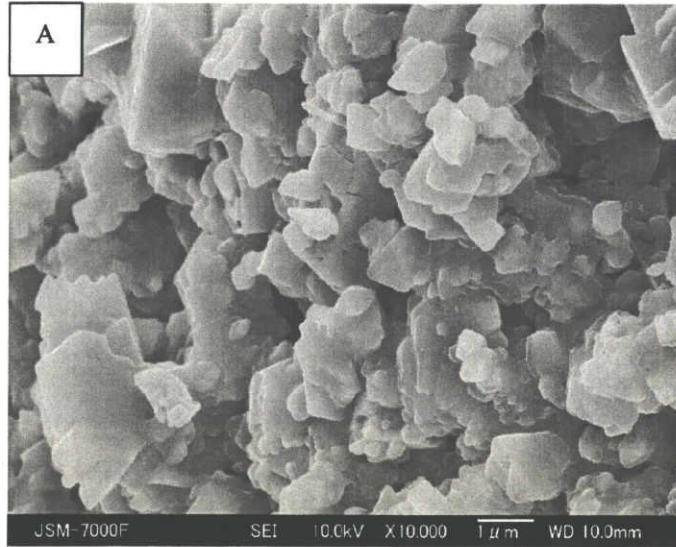


Figure 3.3 SEM images of unwashed and washed sample using the distilled water (A-unwashed; B-washed)

3.4 Influence of reaction temperature on the formation of ZnO microtubes



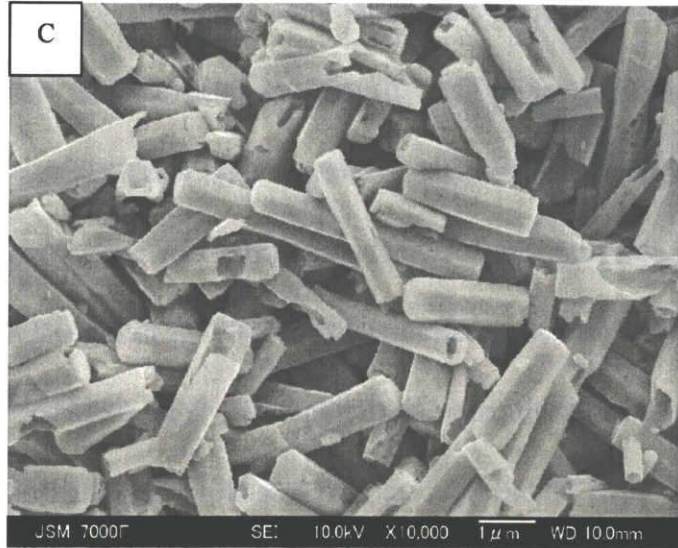


Figure 3.4 SEM images of ZnO particles synthesized at different reaction temperature (A-70 °C; B-80 °C; C-90 °C).

Table 3.1 the effect of reaction temperature on the length, diameter aspect ratio of ZnO microtubes

Reaction Temperature (°C)	Length (μm)	Diameter (nm)	Aspect ratio
70			
80	2.0	600	3.3
90	2.5	500	5

The temperature-dependent experiments at 70 °C, 80 °C and 90 °C were carried out for synthesis of ZnO particles, of which SEM images were shown in Figure 3.4. When the reaction temperature was 70 °C, irregular particles rather than ZnO microtubes were formed, as shown in Figure 3.4 (A). This indicates that activation energy barrier for the formation of ZnO microtubes can not be overcome at this temperature. When the reaction temperature was over 80 °C, hexagonal ZnO microtubes were obtained, as shown in Figure 3.4 (B) and (C). With the reaction temperature increase from 80 °C to 90 °C, the aspect ratio of length to outer diameter increases from 3.3 to 5, of which the respective length, outer diameter and aspect ratio are shown in Table 3.1. This result indicates that the lower reaction temperature leads to the formation of ZnO microtubes with larger diameters, while the rather higher reaction temperature results in the increase of ZnO microtubes length. For ZnO, the growth rate of each of crystal surfaces is different at various temperatures. At 90 °C, the growth rate of (0001) surface is faster than that at 80 °C, while the growth rate of $\{01\bar{1}0\}$ facets at 80 °C is faster than that at 90 °C. One possible reason is that with increasing reaction temperature, the size of growth units should increase, which results in the decrease of the adsorption rate of growth units on $\{01\bar{1}0\}$ facets at 90 °C. While (0001) surface possesses the highest energy, the size of the growth units has a little effect on the adsorption rate of growth units on (0001) surface. The bigger growth units lead to the higher growth rate along [0001] direction at 90 °C. Therefore, the different aspect ratio of ZnO microtubes formed at different temperatures is attributed to a different crystal

growth rate along certain crystal faces due to the effects of temperature on the crystal growth habit. Hence, the reaction temperature has an important role in the growth rate of different facets. Moreover, the structure of ZnO particles synthesized at 90 °C is completely regular hexagonal shape compared with that formed at 80 °C, which is due to the lower growth rate of $\{01\bar{1}0\}$ facets at 90 °C. It is shown that the temperature not only has a great influence on the morphology of ZnO particles but also affects the size of ZnO microtubes slightly. Therefore, the reaction temperature is an important factor for a controllable synthesis of ZnO particles.

3.5 Investigation of aging duration-dependence experiments

To investigate the growth mechanism of ZnO microtubes, in the present study, aging duration-dependent experiments were successfully carried out, and their morphologies from the initial stage to ZnO microtubes were recorded by SEM. The crystal growth process of ZnO tubes can be divided into two stages – the formation of rod-like particles and transition from rod-like to tube-like particles. At the same time, the compositions of the wet precipitate at different aging time were analyzed using XRD.

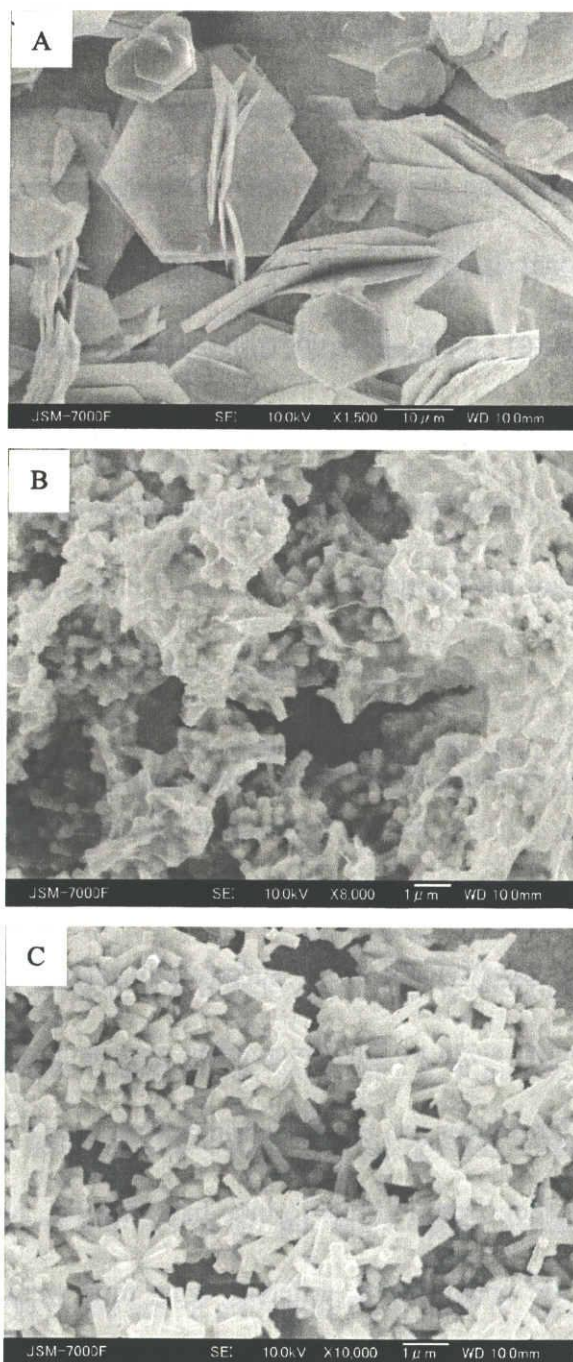
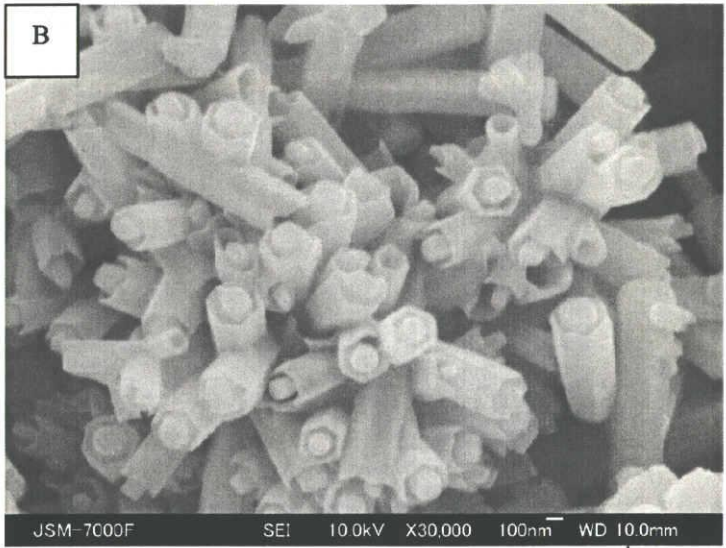
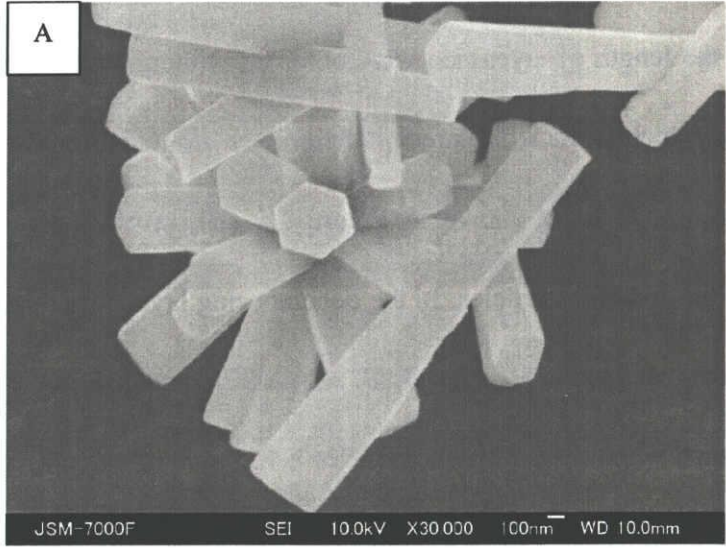


Figure 3.5 SEM images of morphological evolution from layer-like to rod-like particles with different aging duration. (A) – 0 h; (B) – 2 h; (C) – 6 h.

Figure 3.5 reveals the morphological evolution of ZnO particles adjusting the aging duration at the first stage. It can be clearly seen that layer-like particles with 10~12 μm in the length of layer-side were obtained without aging duration, shown in Figure 3.5 (A), which is the white precipitate directly filtrated after the reaction. While aging duration was 2 h, as shown in Figure 3.5 (B), layer-like particles began to decomposing into rod-like particles. In the decomposing layer structure, it is likely that some of rod-like just grow up. Figure 3 (C) shows SEM image of well hexagonal ZnO microrods formed when the aging duration for 6 h. Some of hexagonal rods assemble together and form flower-like structure.



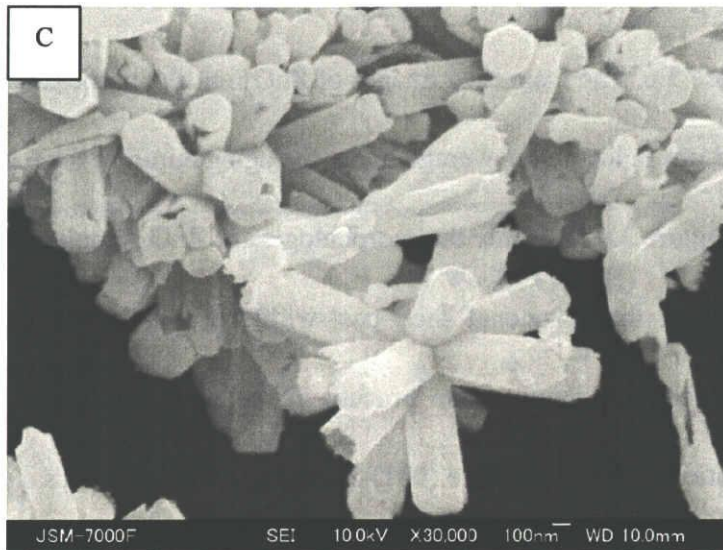


Figure 3.6 SEM images of morphological evolution from rod-like to tube-like particles with different aging duration. (A) – 6 h; (B) – 3 days; (C) and (D) – 3 months.

Morphological evolution from rod-like to tube-like particles at the second stage is shown in Figure 3.6. The magnified images of ZnO rod-like particles with 400 nm in diameter and 1.5 μm in length on average under the aging duration for 6 h are shown in Figure 3.6 (A). Figure 3.6 (B) show the morphologies of ZnO samples obtained after 3 days aging duration, the hexagonal shell peel with the column-like particles inside, which is the evidence of intermediate process in the second stage. The preferential chemical dissolution of the metastable (001)-Zn faces of the microrods shall lead to the tubular ZnO particles, as shown in Figure 3.6 (C). The aging duration is such that the systems will tend to reach their thermodynamic stability and may therefore undergo variations of morphology, size and structure properties. [3]

Figure 3.7 shows XRD patterns of wet products with different aging time. The precipitates were filtrated and then analyzed using XRD. The products without aging duration are the hydrate of zinc oxide precursor. With the aging time increasing, the precursors turn into zinc oxide. Until the aging time is 8 h, the products still contain some precursor except zinc oxide. From the SEM images, when the aging time is over 6 h, the morphology of products is rod-like particles. These imply the rod-like particles still contain some hydrate of zinc oxide precursor.

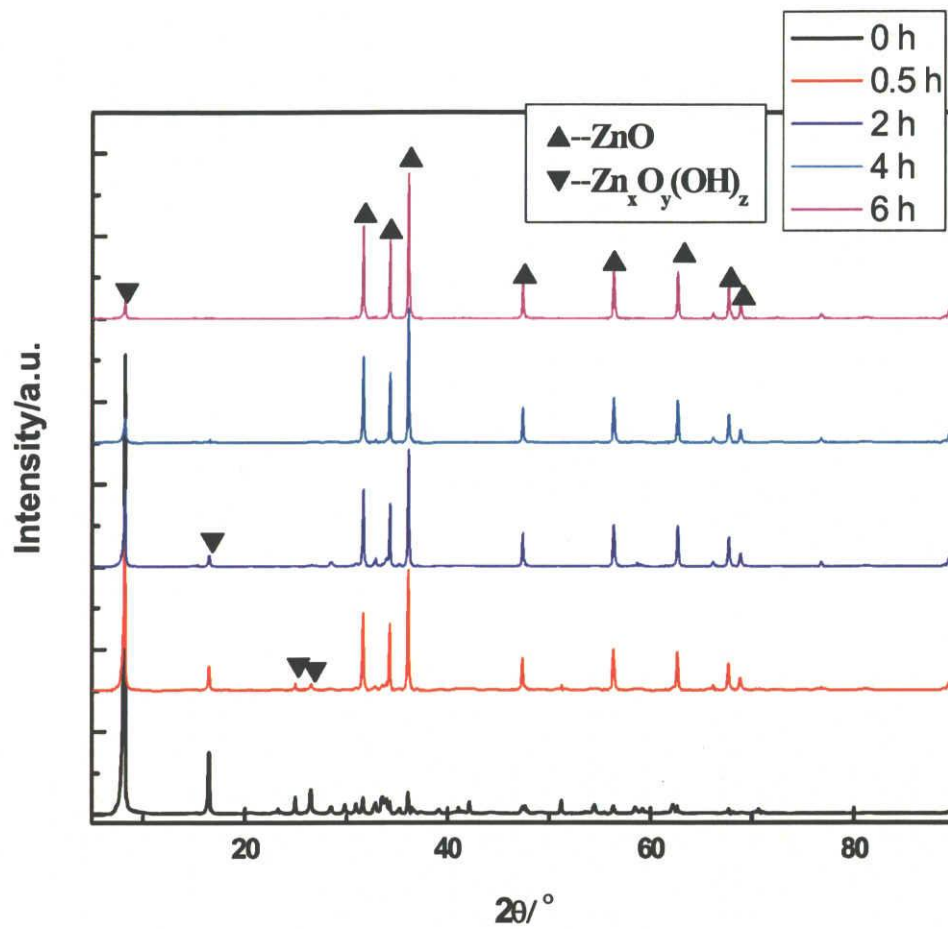


Figure 3.7 XRD patterns of wet products with different aging time

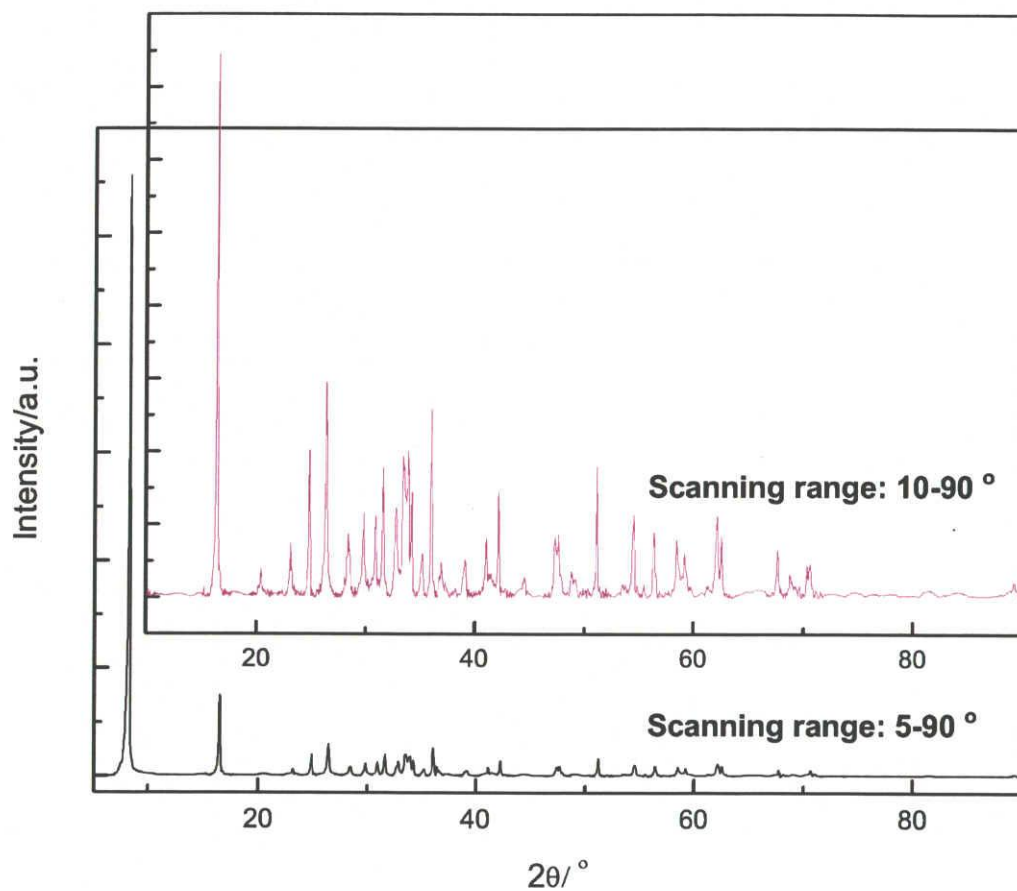


Figure 3.8 XRD patterns of wet precursor scanning range from 5 ° to 90 ° and from 10 ° to 90 °

XRD patterns of wet precursor scanning range from 5 ° to 90 ° and from 10 ° to 90 ° are shown in Figure 3.8. Compared with the sample dried at room temperature, the composition of wet precursor is almost as same as the products dried at room temperature. The wet precursors are the compound of several kinds of zinc oxide

hydrate.

3.6 Growth mechanism of ZnO microtubes via the aqueous solution process

The growth habit of crystal is related to the relative growth rate of various crystal faces bounding the crystal. The difference of the growth rate of various crystal faces results in different growth habits. Under the aqueous solution, the diffusion of ions and complex is not the main factor affecting the growth rate, so the growth rate of various crystal faces is mainly related to their surface energy.

The growth process of ZnO microtubes at the aqueous solution has been discussed briefly. The conditions of the aqueous solution can be controlled by adjusting growth temperature and the pH. Meanwhile, the crystal phase of the precipitate was mainly determined by the pH of the aqueous solution. If the pH was in the range 7 to 8, the obtained precipitate formed the wurtzite ZnO crystal. In the progress of the formation of ZnO, the growth units $[\text{Zn}(\text{NH}_3)_4]^{2+}$ and $[\text{Zn}(\text{OH})_4]^{2-}$ [4-7] encapsulated by water were formed first. These growth units are easy to attach on the surface of precipitate. The formation of hexagonal rod-like particles is attributed to the different growth rate of the various crystal facets and the polar (0001) surface. The relative growth rate of these crystal surfaces, which can be adjusted by the growth conditions, will determine the aspect ratio of ZnO microtubes. Generally, the growth rate of ZnO crystal in the aqueous solution in the [0001] direction is about twice as fast as that in the $\langle 01\bar{1}0 \rangle$ direction. [8] That is due to (0001) surface has roughly a 60 % higher

cleavage energy than the nonpolar $\{01\bar{1}0\}$ facets [9], which results in the higher growth rate along the $[0001]$ direction with the formation of unstable surface. According to classical crystal growth theory, a crystal facet grows rapidly, and easily disappears from the final crystal morphology. Finally ZnO microtubes were formed by the dissolution of unstable (0001) surface. Figure 3.9 shows schematic illustration of possible growth mechanism for ZnO microtubes.

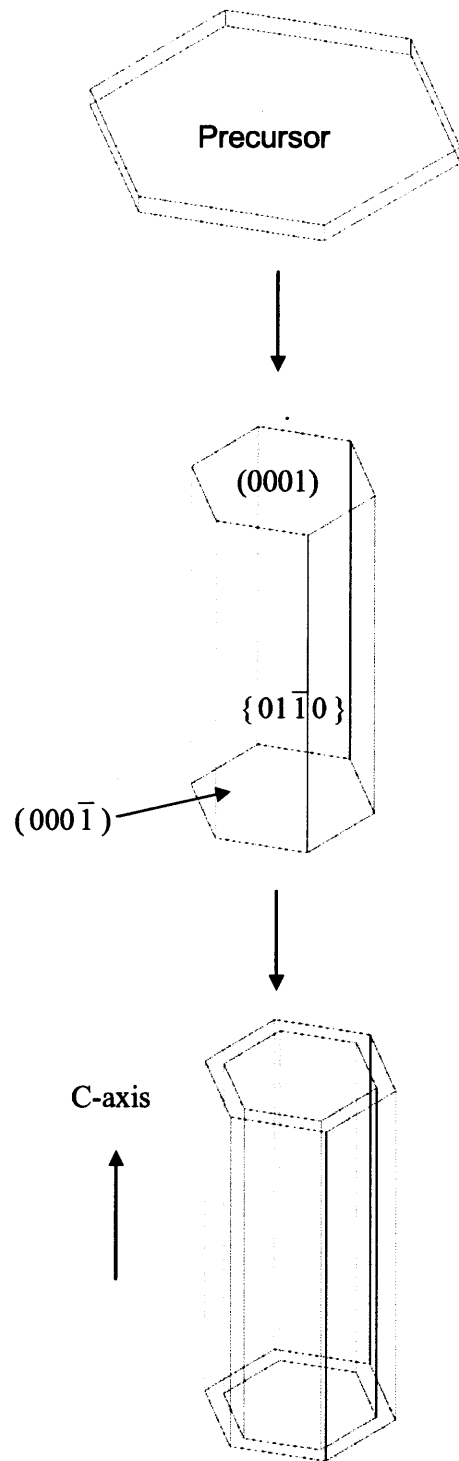


Figure 3.9 Schematic illustration of possible growth mechanism for ZnO microtubes

3.7 Synthesis of ZnO nanotube

In order to control the size of ZnO microtubes and synthesize ZnO nanotubes, many attempts have been performed so far by adjusting various influence factors, such as the concentration of zinc ions, reaction temperature and aging time. ZnO nanotubes have been synthesized at reaction temperature 70 °C. The zinc ionic concentration of zinc chloride aqueous solution (400 ml) is 0.25 M and the final pH value is 7.5. After stop the introduction of ammonia water, the reaction solution was maintained at 70 °C for 3 h. Then the white precipitate were filtrated and dried at 90 °C for 24 h, as shown in Table 3.2.

Table 3.2 Conditions for synthesis of ZnO nanotubes

Zn ²⁺ concentration	pH	Reaction Temp.	Drying Temp.	Keeping Time	Keeping Temp.
0.25 M	7.5	70 °C	90 °C	3 h	70 °C

Figure 3.10 shows SEM images of ZnO nanotubes synthesized at 70 °C with 0.25 M the concentration of zinc ions. The nanotubes have a uniform outer diameter of 80-100 nm, 600-900 nm long and the wall thickness of 10 nm, as shown in Figure 3.10 (B).

Two important factors are dealt with in this study: the dimension of growth units and the effect of reaction temperature on the different surface energy. At the lower concentration of zinc ions, the dimension of growth units is lower. The growth rates on different crystal surface as well as in different temperature are distinct. At lower temperature, the surface energy should decrease, which results in the decrease of the adsorption rate of growth rate on $\{01\bar{1}0\}$ facets. Meanwhile, in the 0.25 M zinc chloride aqueous solution and at 70 °C, the size of growth units is smaller than that in the 0.5 M or at higher temperature. The surface energy has a more significant influence on the growth rate than the growth units. The growth rates on $\{01\bar{1}0\}$ facets decrease, which is mainly attributed to the surface energy. While (0001) surface still possesses the highest energy although it decreases, however the size of growth units decreases, there has a little effect on the growth rate along [0001] direction.

It is evident from the above experimental results that adjustment among the parameters is an effective way to design and synthesize tubular nanostructure of ZnO in dimensions ranging from nanometers to micrometers.

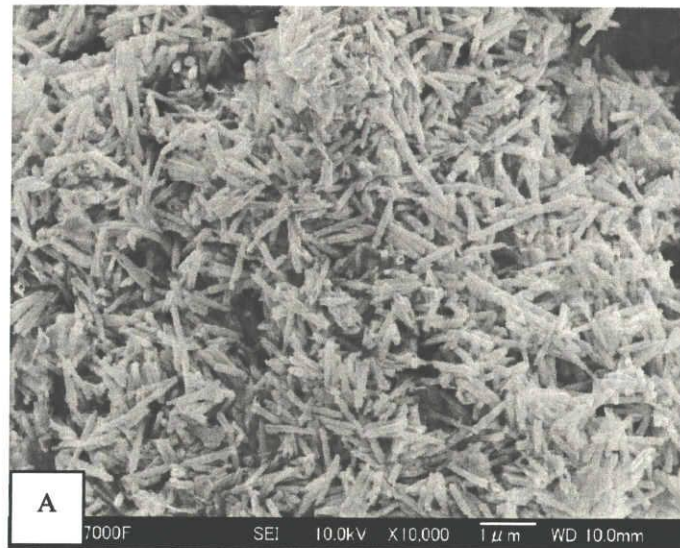


Figure 3.10 SEM images of ZnO nanotubes synthesized at 70 °C with the concentration of zinc ions 0.25 M

3.8 Percentage of synthesized ZnO tubes and yield of product

From now, ZnO microtubes and nanotubes have been fabricated via the aqueous solution process. Figure 3.11 shows the highest percentage of synthesized ZnO microtubes. The percentage of ZnO tube is over 90 % from the broken particles, as shown in Figure 3.11 (B).

In our study, when the pH value is 7.5 and zinc chloride aqueous solution is 400 ml, of which zinc ionic concentration is 0.5 M, the average yield of ZnO microrods or microtubes is 9.5 g. This yield is less than the theoretical value 16.2 g, which is caused by loss of filtration and drying processes and dissolution of zinc complex in the reaction solution.

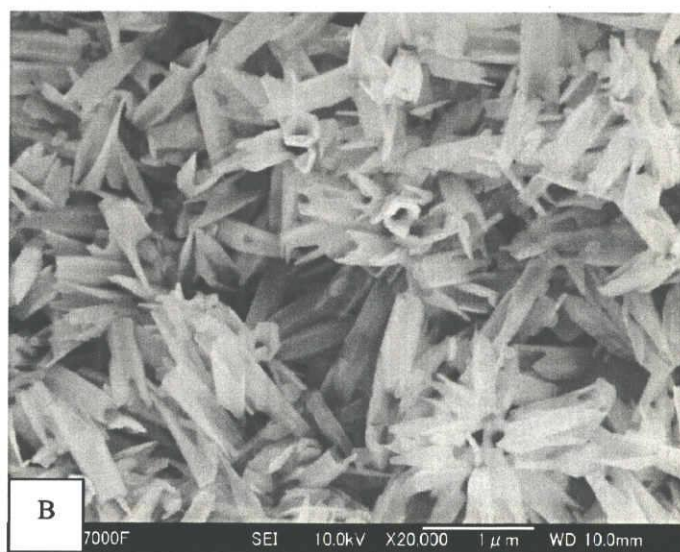
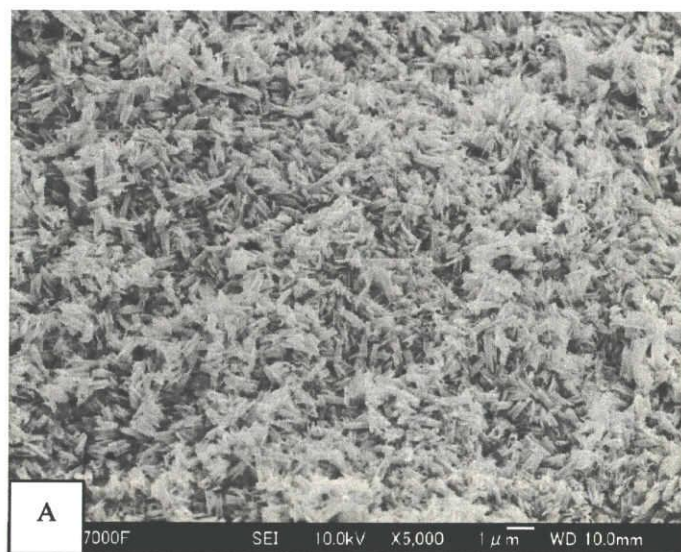


Figure 3.11 SEM images of highest percentage of synthesized ZnO microtubes

3.9 Conclusion

This chapter investigated the synthesis of ZnO micro- and nano- particles with tubular structure, which involved the introduction of ammonia water into the zinc chloride aqueous solution. This study has the good effect of simpleness, novelty, safety, easy operation, economy, large-scale production.

The influence of reaction temperature on the morphologies of ZnO samples was discussed. The results show that the temperature not only has obvious influence on the morphology but also affect the size slightly. With temperature increase from 80 °C to 90 °C, the aspect ratio of the length to the outer diameter increase from 3.3 to 5.

Through adjusting the concentration of zinc ions, reaction temperature, aging duration, ZnO nanotubes with uniform outer diameter of 80-100 nm, length of 600-900 nm and the wall thickness of 8-10 nm have been successfully fabricated. It is a breakthrough of the aqueous solution technique for synthesis of ZnO particles with tubular structure.

The morphological evolution with the aging duration has been successfully obtained. Based on the investigated results, the growth mechanism of ZnO microtubes has been proposed. The formation of tubes is attributed to the different growth rate of each facet. The fast growth of [0001] direction cause this surface unstable and dissolution in the later reaction, resulting in the formation of hexagonal tubular structure.

Also, it is shown that the highest percentage of synthesized ZnO microtubes is over 90 % and the average yield of ZnO microrods or microtubes is 9.5 g, when the pH value is 7.5 and zinc chloride aqueous solution is 400 ml, of which zinc ionic concentration is 0.5 M.

Reference

- [1] Anli Yang, Zuolin Cui, "ZnO layer and tubular structures synthesized by a simple chemical solution route", *Mater. Lett.*, MLBLUE-06877 (2006).
- [2] Z. Wang, X.F. Qian, J. Yin and Z.K. Zhu, "Large-Scale Fabrication of Tower-like, Flower-like, and Tube-like ZnO Arrays by a Simple Chemical Solution Route", *Langmuir*, 20 3441-3448 (2004).
- [3] Lionel Vayssieres, Karin Keis, Anders Hagfeldt and Sten-Eric Lindquist, "Three-Dimensional Array of Highly Oriented Crystalline ZnO microtubes", *Chem. Mater.*, 13 [12] 4395-4398 (2001).
- [4] K. Govender, D.S. Boyle, P.B. Kenway and P.O'Brien, "Understanding the factors that govern the deposition and morphology of thin films of ZnO from aqueous solution", *J. Mater. Chem.*, 14 2575-2591 (2004).
- [5] J. Zhang, L. D. Sun, J. L. Yin, H. L. Su, C. S. Liao, and C. H. Yan, "Control of ZnO morphology via a simple solution route", *Chem. Mater.*, 14 (2002), 4172-4177.
- [6] S. Yamabi and H. Imai, "Growth conditions for wurtzite zinc oxide films in

aqueous solution”, *J. Mater. Chem.*, 12 (2002), 3773-3778.

[7] Z. Wang, X. F. Qian, J. Yin, Z. K. Zhu, “Aqueous solution fabrication of large-scale arrayed obelisk-like zinc oxide nanorods with high efficiency”, *J. Solid State Chem.*, 177 (2004), 2144-2149.

[8] R.A. Laudise and A.A. Ballman, “Hydrothermal Synthesis of Zinc Oxide and Zinc Sulfide”, *J. Phys. Chem.*, 64 688-691 (1960).

[9] B.Meyer and D. Marx, “Density-functional Study of the Structure and Stability of ZnO Surface”, *Phys. Rev. B*, 67 035403 (2003).

**CHAPTER 4 PHOTOLUMINESCENCE PROPERTY AND
X-RAY PHOTOELECTRON SPECTROSCOPY ANALYSIS**

4.1 Introduction

Luminescence is a nonequilibrium process for it needs excitation source, such as lamp or laser. Depending on the different excitation source, it can be divided into photoluminescence (PL), which requires optical excitation, electroluminescence (EL), which needs excitation by electrical current, cathodoluminescence (CL), which results from electron bombardment, and the other kinds of luminescence. PL is one of most widely used experimental methods for study of semiconductors, especially wide-band-gap material.[1-6] Until now, there has been a huge interest in the wide-band-gap material ZnO. It is mainly due to the fact that ZnO might be a viable alternative to GaN as ultraviolet light source [7] and the hope to obtain a ferromagnetic semiconductor at room temperature [8] for spintronic devices. A lot of attention has been attracted by a multitude of ZnO structure, which is the scientific prospect. The optical properties are mainly governed by impurities, crystal quality and surface properties. The surface play a significant role in the process of the luminescence and the surface states will have profound effect on the luminescence properties.

In order to investigate the photoluminescence properties of as-synthesized ZnO microtubes via the developed aqueous solution method, PL techniques were carried out. The green and blue emissions have been frequently reported, which is caused by defects such as oxygen vacancies, zinc vacancies, interstitial zinc and antisite oxygen. There are few literatures about the orange-red emission of ZnO microtubes. And the chemical

state of zinc and oxygen on the surface of ZnO microtubes were studied by the XPS analysis to explain the mechanism of the PL property.

4.2 Experimental procedure

The photoluminescence characteristics of ZnO tubes were investigated by photoluminescence measurement using a spectrofluorometer (JASCO FP-6500), which use an excitation wavelength of 340 nm. The phase composition was investigated by X-ray photoelectron spectroscopy (XPS) on a SSX-100 (Surface Science Instrument) instrument. A monochromatic Al $K\alpha$ x-ray radiation was used as excitation source in the XPS measurement. The energy resolution of the instrument at 20 eV is 0.05 eV as estimated from the full width at half maximum of the XPS Ag $3d_{5/2}$ of a pure silver target. The emitted photoelectrons were detected using a hemispherical analyzer at pass energy of 20 eV for the C 1s high resolution XPS peaks.

The annealing treatment of ZnO tubes were carried out using an Infrared Image Furnace (MS-E44-AN, ULVAC SINKU-RIKO, Yokohama, Japan) for 2 h in air. The temperature increasing rate and decreasing rate are controlled by a temperature program controller, which are 10 °C/min (TPC-1000, ULVAC, Japan).

4.3 Results and Discussion

4.3.1 Photoluminescence analysis

Figure 4.1 is the room temperature photoluminescence spectrum of ZnO microtubes without annealing treatment. PL spectrum possesses a visible emission band. The visible emission centered at about 582 nm ranging from 400 nm to 660 nm, which is associated with oxygen vacancies. The broadening of the visible emission can be ascribed to abundant surface defects. A large quantity of defects and impurities at the surface of ZnO microtubes can provide new states which can contribute as visible luminescence centers and broaden the visible emission band. [9]

Figure 4.2 shows PL spectrum of ZnO microtubes annealed for 2 h at 600 °C in air. When ZnO nanotubes are annealed in air, the number of oxygen vacancies in ZnO microtubes will decrease. As the result, the oxygen vacancy-related visible emission intensity decrease, leading to the visible emission center position shifting from 582 nm to 612 nm, which is attributed to the surface defect-related visible emission intensity. Compared with the standard PL spectrum of ZnO nanoparticles (20 nm) (Wako Ltd., Japan), as shown in Figure 4.3, the visible emission intensity is stronger. On the other hand, in Figure 4.4, the SEM images show that the annealed ZnO microtubes have smooth surface, but almost all of ZnO tubes are broken.

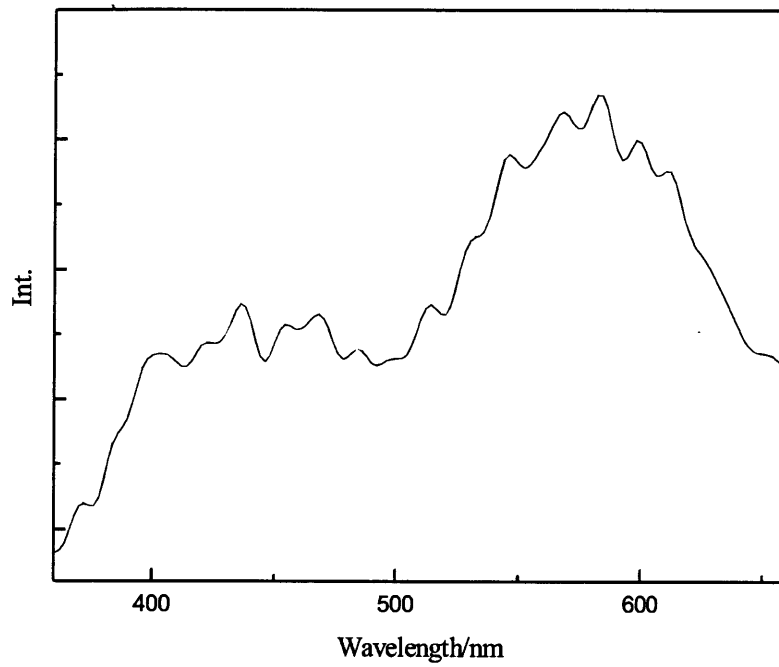


Figure 4.1 Photoluminescence spectrum of ZnO microtubes without annealing treatment

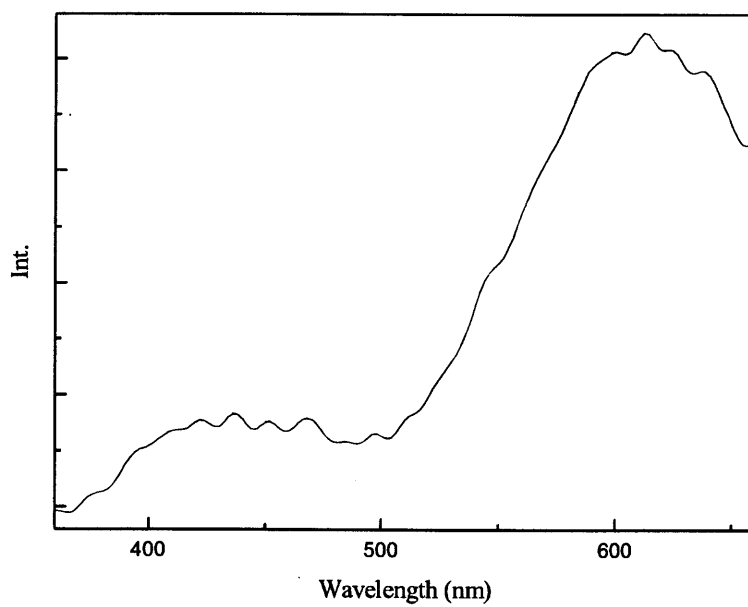


Figure 4.2 Photoluminescence spectrum of ZnO microtubes annealed at 600 °C for 2 h in air

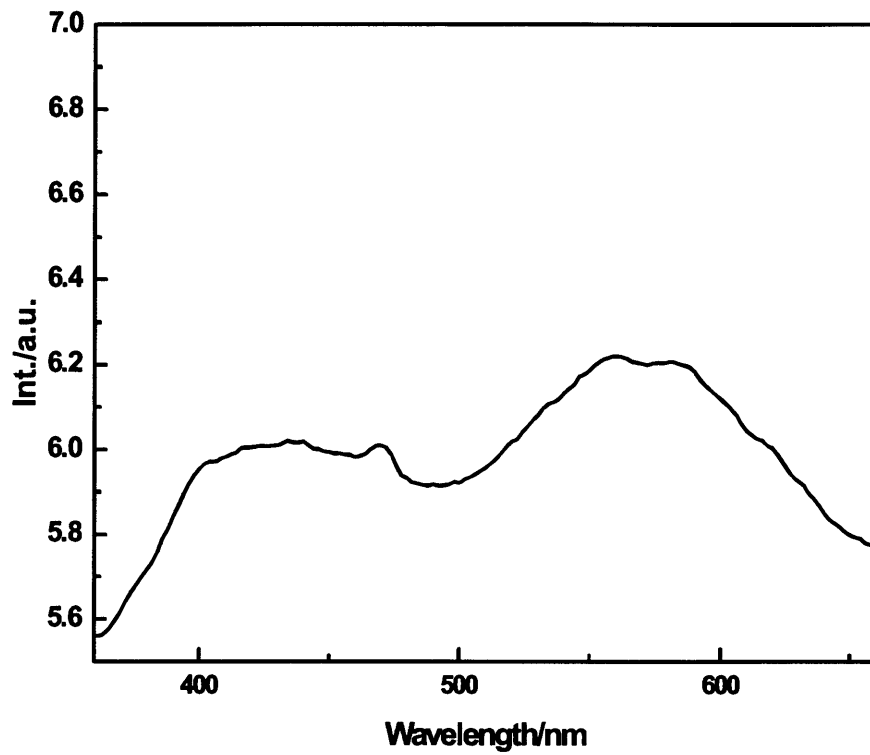


Figure 4.3 Photoluminescence spectrum of ZnO nanoparticles (20 nm) from Wako Ltd.

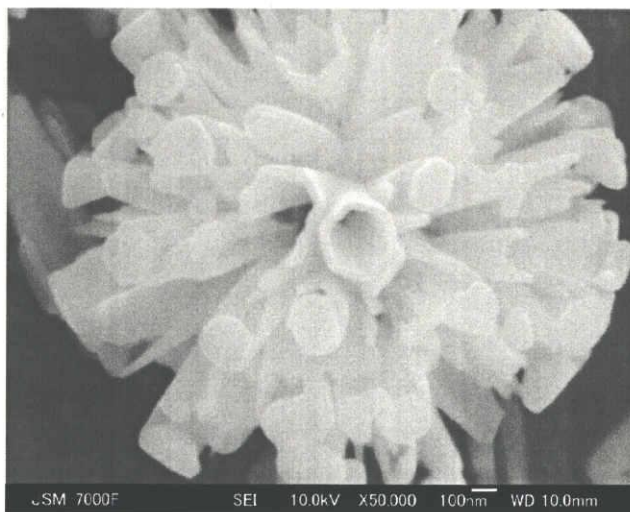
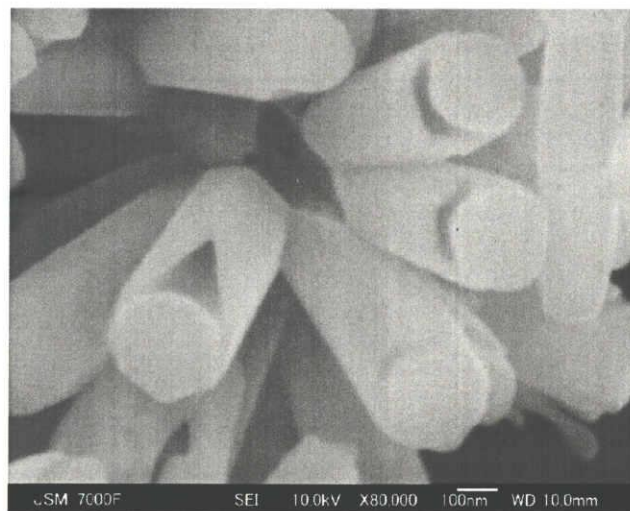


Figure 4.4 SEM images of ZnO tubes with the annealing treatment

4.3.2 X-ray photoelectron spectroscopy (XPS) analysis of ZnO microtubes

A broad scan survey spectrum is obtained to identify the elements in ZnO microtubes. Figure 4.5 shows a typical wide-scan spectrum of as-synthesized ZnO microtubes. The photoelectron peaks of the main elements, Zn and O, were obtained. No other impurities were detectable in the XPS spectrum. From the statistical results of XPS, as shown in Table 4.1, the atom ratio of zinc to oxygen is about 2.67 for ZnO microtubes without annealing treatment, which shows that ZnO microtubes are zinc-rich. There are two main reasons: one is that there exist many oxygen vacancies on the surface of ZnO microtubes; another is that zinc ions and zinc soluble complexes were adhered onto the surface of ZnO microtubes during the drying process. Zinc composition of ZnO microtubes decreases from 72.8 % to 41.6 % after annealing treatment, while oxygen composition of ZnO microtubes increases from 27.2 % to 58.4 %. ZnO microtubes turn into oxygen-rich particles from zinc-rich particles. When the samples were annealed at 600 °C in air, zinc ions on the surface of ZnO tubes are easier to be oxidized. At the same time, there are many surface-defects formed.

Table 4.1 Composition of ZnO microtubes before and after annealing treatment

	Without annealing	Annealed at 600 °C for 2 h
Zn atom percentage (%)	72.8	41.6
O atom percentage (%)	27.2	58.4
Zn/O	2.67	0.71

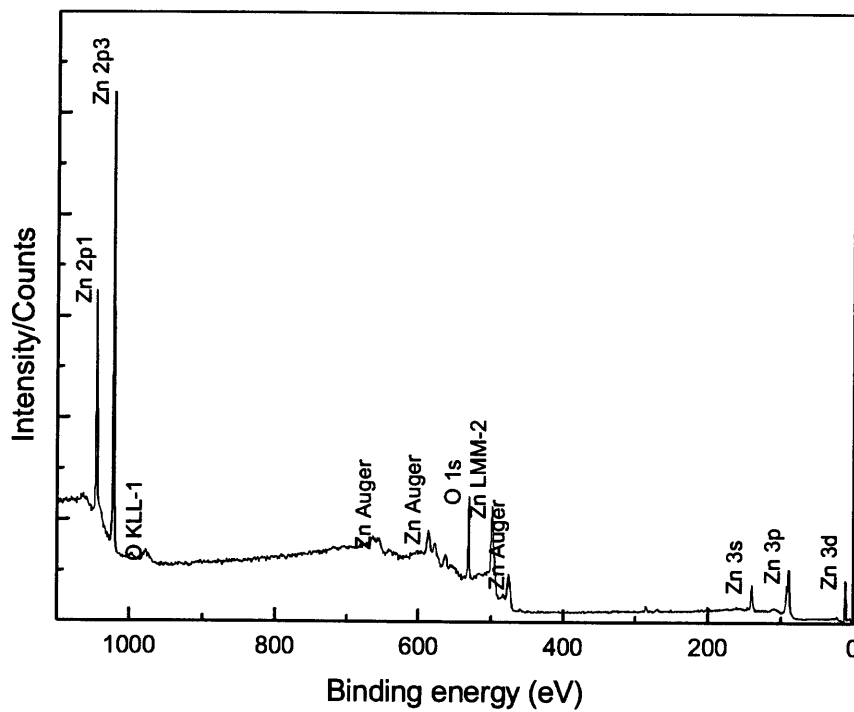


Figure 4.5 The survey scan spectrum of ZnO microtubes

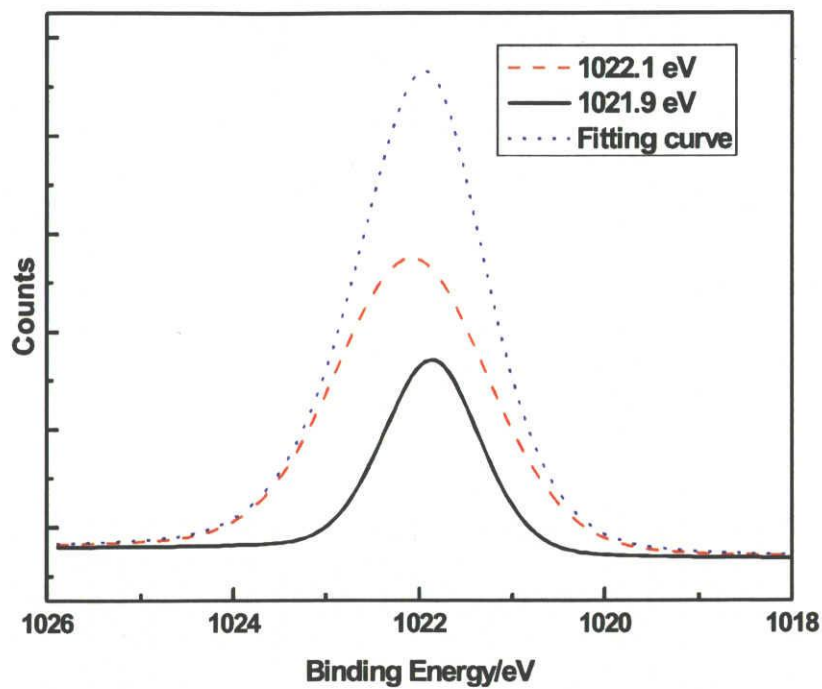


Figure 4.6 Zinc 2p₃ spectra of ZnO microtubes

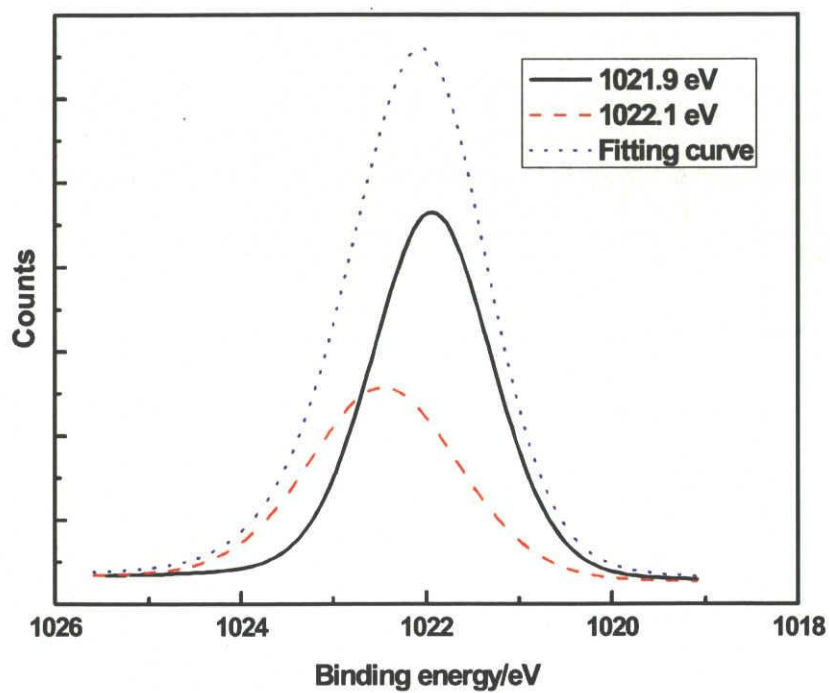


Figure 4.7 Zinc 2p₃ spectra of ZnO microtubes with the annealing treatment at 600 °C for 2 h

The XPS spectra of ZnO microtubes exhibit two binding energy of Zn-2p_{3/2} located at 1022.1 eV and 1021.9 eV, corresponding to Zn-Cl bonds and Zn-O bonds separately, as shown in Figure 4.6. Zinc ions attached on the surface of ZnO microtubes are responsible for the binding energy peak to be positioned at 1022.1 eV. Because after evaporation, zinc ions and chloride ions are attached on the surface of ZnO microtubes and the depth of XPS analysis is 0.1-5 nm, the peak of binding energy of 1022.1 eV is higher than that of 1021.9 eV. During the annealing treatment, zinc ions were very easy to be oxidized and finally formed zinc oxide, which is responsible for the increase of the binding energy peak of 1021.9 eV and the decrease of the binding energy peak of 1022.1 eV, as shown in Figure 4.7. Before the annealing treatment, the surface of ZnO microtubes is zinc-rich, exist oxygen vacancies, PL property is the oxygen vacancy-related visible emission. When ZnO microtubes were annealed, the number of oxygen vacancies in the surface of ZnO microtubes will decrease. On the other hand, the surface defects of the annealed ZnO microtubes increase. As a result, the oxygen vacancy-related visible emission intensity decreases while surface defect-related visible emission intensity increases, leading to the redshift of the visible emission center.

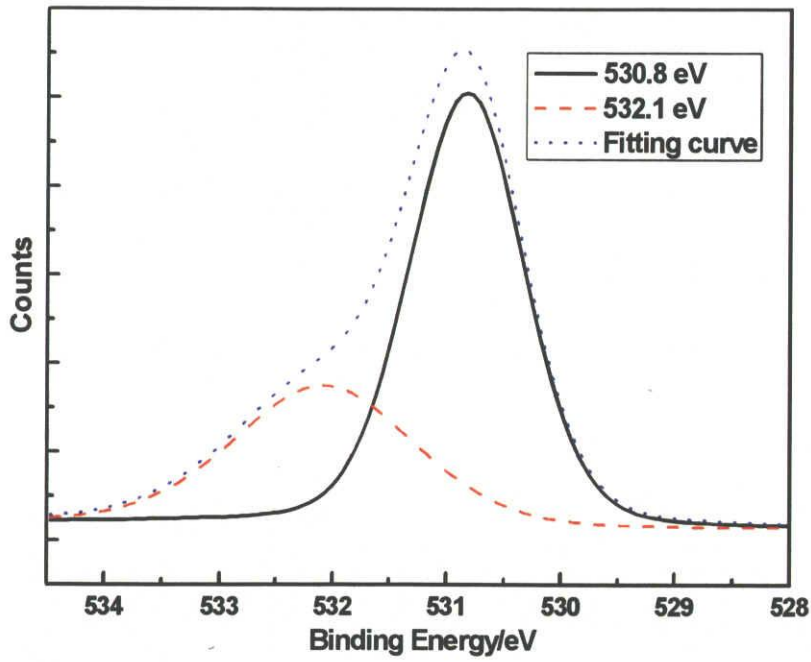


Figure 4.8 Oxygen 1s spectra of ZnO microtubes

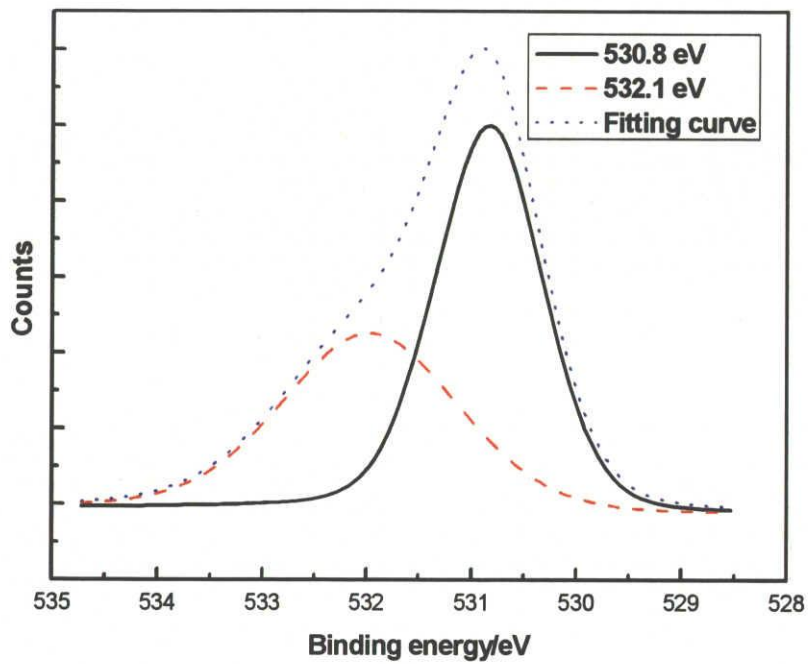


Figure 4.9 Oxygen 1s spectra of ZnO microtubes with annealing treatment at 600 °C for 2 h

The typical O 1s peaks in the surface of ZnO microtubes can be consistently fitted by Gaussian, which contains a strong peak at 530.8 eV and a weak peak at 532.1 eV, as shown in Figure 4.8 and Figure 4.9. The component on the low and strong binding energy side of the O 1s spectrum at 530.8 eV is attributed to O²⁻ ions on the wurtzite structure of hexagonal Zn²⁺ ion array in the Zn-O bonds. The peak related to the high binding energy around 532.1 eV is attributed to the presence of chemisorbed or dissociated oxygen and OH species on the surface of ZnO microtubes. From the Oxygen 1s spectra of ZnO microtubes without and with annealing treatment at 600 °C for 2 h, it also can conclude that the surface-defects increase after the annealing treatment.

4.4 Conclusion

The chemical composition of ZnO microtubes, based on XPS results, reveals that the concentration of oxygen increase after annealing treatment, that is to say, the oxygen vacancies decrease. The oxygen vacancy-related visible emission intensity decreases, while the surface defect-related visible emission intensity increases, leading to the visible emission center position shifting from orange emission 582 nm to red emission 612 nm.

Reference

- [1] X. J. Yang, X. Y. Miao, X. L. Xu, C. M. Xu, J. Xu, H. T. Liu, "Structure, X-ray photoelectron spectroscopy and photoluminescence properties of highly ordered ZnO microrods", *Opt. Mater.*, 27 (2005), 1602-1605.
- [2] J. Antony, X. B. Chen, J. Morrison, L. Bergman and Y. Qiang, "ZnO nanoclusters: Synthesis and photoluminescence", *Appl. Phys. Lett.*, 87 (2005), 241917.
- [3] P. T. Hsieh, Y. C. Chen, K. S. Kao, C. M. Wang, " Luminescence mechanism of ZnO thin film investigated by XPS measurement", *Appl. Phys. A*, 90 (2008), 317-321.
- [4] M. Yoneta, K. Yoshino, M. Ohishi, H. Saito, "Photoluminescence studies of high-quality ZnO single crystals by hydrothermal method", *Physica. B*, 376–377 (2006), 745–748
- [5] S.J. Chen, Y.C. Liu, Y.M. Lu, J.Y. Zhang, D.Z. Shen, X.W. Fan, "Photoluminescence and Raman behaviors of ZnO nanostructures with different morphologies", *J. Crys. Growth*, 289 (2006), 55-58.
- [6] P. Zu, Z. K. Tang, G. K. L. Wong, M. Kawasaki, A. Ohtomo, H. Koinuma, Y. Segawa, "Ultraviolet spontaneous and stimulated emission from ZnO microcrystallite thin films at room temperature", *Solid State Commun.*, 103 (1997), 459-463.
- [7] A. Tsukazaki, T. Onuma, M. Ohtani, T. Makino, M. Sumiya, K. Ohtani, S. F. Chichibu, S. Fuke, Y. Segawa, H. Ohno, H. Koinuma and M. Kawasaki, "Repeated

- temperature modulation epitaxy for p-type doping and light-emitting diode based on ZnO”, *Nat. Mater.*, 4 [1] (2005), 42-46.
- [8] T. Dietl, H. Ohno, F. Matsukura, J. Cibert and D. Ferrand, “Zener model description of ferromagnetism in zinc-blende magnetic semiconductors”, *Science*, 287 (2000), 1019-1022.
- [9] Yanhong Tong, Yichun Liu, Changlu Shao, Yuxue Liu, Changshan Xu, Jiying Zhang, Youming Lu, Dezhen Shen and Xiwu Fan, “Growth and Optical Properties of Faceted Hexagonal ZnO Nanotubes”, *J. Phys. Chem. B*, 110 (2006), 14714-14718.

CHAPTER 5 SUMMARY

In this study, a large quantity of well-crystalline ZnO nano- and micro-hexagonal tubes with well-defined crystallographic faces have been directly synthesized via a facile and new aqueous solution method through introducing ammonia water (bubbles) into zinc chloride aqueous solution under the relative low temperature (90 °C) and atmospheric normal pressure, which performed in a glass flask. This research is particularly taking advantage of easy control, large-scale production, low cost, et al.

ZnO microtubes presents the diameter in the range of 300 nm-500 nm, and the thickness of wall 30-50 nm, the length of the tubes 1-2.5 μm on average, which are synthesized at reaction temperature 90 °C, the concentration of starting zinc ions 0.5 M, the final pH value 7.5, and dried at 90 °C for 24 h.

Through adjusting the concentration of zinc ions, reaction temperature, aging duration, ZnO nanotubes with uniform outer diameter of 80-100 nm, length of 600-900 nm and the wall thickness of 8-10 nm have been successfully fabricated, which are synthesized at reaction temperature 70 °C, the concentration of zinc ions 0.25 M, the final pH value 7.5, and dried at 90 °C for 24 h.

The external parameters, such as pH, drying conditions, reaction temperature, aging process, integrate to dominate the synthesis process, which have been investigated separately. The growth mechanism has been proposed based on the above investigated results.

Chapter 1 presents the properties and applications of ZnO particles, the crystal structure and special growth structure of ZnO, and the conventional techniques for the

fabrication in order to clarify the background of this study. Accordingly, the goal of this study was described.

In chapter 2, well-crystalline hexagonal ZnO microtubes were successfully synthesized via an aqueous solution process through the introduction of ammonia bubbles into zinc chloride solution. The influence of the final pH value on the formation of ZnO microtubes was discussed. The initial thought for growth mechanism is using ammonia bubbles as templates; and then the optimization of drying process was systematically carried out. From this research, it can be get that the ammonia bubbles is not the template for the formation of ZnO microtubes, but just as the reactant, which step further in proposing the formation mechanism. In order to investigate the growth mechanism and simplify the experimental procedure, continue to study the following chapter 3.

In chapter 3 investigated the synthesis of ZnO microtubes using the ammonia water instead of ammonia bubbles in the aqueous solution, which is easier to control. The effects of ammonia and reaction temperature were discussed in this chapter. In order to get the evidence of the intermediate morphologies, systematical aging duration-dependent experiments were compared comprehensively to reveal the formation and detailed growth process of ZnO particles with tubular structure. Based on the results and the special ZnO crystal property, the mechanism of the formation of ZnO tubes was proposed. Also, through adjusting the reaction temperature, the starting concentration of zinc ions, aging time and temperature, ZnO nanotubes were

successfully fabricated via the developed aqueous solution method. It is a breakthrough of the aqueous solution approach for synthesis of ZnO particles with tubular structure.

In chapter 4, the chemical composition of ZnO microtubes, based on XPS results, reveals that the concentration of oxygen increase after annealing treatment, that is to say, the oxygen vacancies decrease. The oxygen vacancy-related visible emission intensity decreases, while the surface defect-related visible emission intensity increases, leading to the visible emission center position shifting from orange emission 582 nm to red emission 612 nm. The orange and red emissions of ZnO microtubes were found in ZnO microtubes via the developed aqueous solution method.

Finally, chapter 5 describes the overall conclusions of the present work.

RESEARCH ACTIVITIES

Publications

Chapter 1

- [1] Liwei Lin, Masayoshi Fuji, Hideo Watanabe and Minoru Takahashi, “Synthesis and potential applications of zinc oxide tubes”, Annual report of the Ceramics Research Laboratory Nagoya Institute of Technology, in preparation.

Chapter 2

- [2] Liwei Lin, Yongsheng Han, Masayoshi Fuji, Takeshi Endo, Hideo Watanabe and Minoru Takahashi, “A facile method to synthesize ZnO tubes by involving ammonia bubbles”, Ceramic Transactions, 198, 269-274, 2007.
- [3] Liwei LIN, Yongsheng HAN, Masayoshi FUJI, Takeshi ENDO, Xiaowei Wang and Minoru TAKAHASHI, “Synthesis of Hexagonal ZnO Microtubes by a Simple Soft Aqueous Solution Method”, Journal of the Ceramic Society of Japan 116[2] 198-200 (2008).
- [4] Yong Sheng Han, Li Wei Lin, Masayoshi Fuji, and Minoru Takahashi, “A Novel One-step Solution Approach to Synthesize Tubular ZnO Nanostructures”, Chemistry Letters, 36, 8, 1002-1003, (2007).

Chapter 3

- [5] Liwei Lin, Hideo Watanabe, Masayoshi Fuji, Takeshi Endo, Seiji Yamashita and Minoru Takahashi, "Synthesis of ZnO Microtubes by a Facile Aqueous Solution Process", Journal of the American Ceramic Society. (In press)
- [6] Liwei Lin, Hideo Watanabe, Masayoshi Fuji and Minoru Takahashi, "Morphological Control of ZnO particles synthesized via a New and Facile Aqueous Solution Route", Advance Powder Technology, 20, 2, 2009. (In press)

Chapter 4

- [7] Liwei Lin, Masayoshi Fuji, Hideo Watanabe and Minoru Takahashi, "Photoluminescence Properties and X-ray Photoelectron Spectroscopy of ZnO Microtubes Synthesized by an Aqueous Solution", Ceramic Transactions. (Submitted).

Other Publications

- [8] Yongsheng Han, Liwei Lin, Masayoshi Fuji, Takeshi Endo, Hideo Watanabe and Minoru Takahashi, "Effect of Surfactants on the Formation of Hollow CaCO₃ Particles by Bubble Template Method", Ceramic Transactions, 198, 263-268, 2007.
- [9] Xiaowei Wang, Yongsheng Han, Liwei Lin, Masayoshi Fuji, Takeshi Endo, Hideo Watanabe and Minoru Takahashi, "A molecular dynamics study on aqueous solutions for preparation of hollow CaCO₃ particles", Modelling Simul. Mater. Sci.

Eng. 16 (2008) 035006 (9pp).

- [10] Seiji Yamashita, Liwei Lin, T. Endo, H. Watanabe, T. Shirai, M. Fuji and M. Takahashi, "Effect of drying conditions on morphology of ZnO particles synthesized by a simple aqueous solution method", *Advance Powder Technology* (Submitted)

Oral/poster presentation

2008

- 1 "Large-scale synthesis of single-crystalline ZnO tubes via a simple solution route" (Oral)

Liwei Lin, Masayoshi Fuji, Takeshi Endo, Seiji Yamashita, Xiaowei Wang and Minoru Takahashi

10th International Conference on Ceramic Processing Science (ICCP-10)

May 25-28, 2008, Inuyama, Japan

- 2 "ZnO Microtubes Synthesized via an Aqueous Solution Method" (Poster)

Liwei Lin, Hideo Watanabe, Masayoshi Fuji, Seiji Yamashita and Minoru Takahashi

The Association of Tokai Young Ceramists 2008

July 10-11, 2008, Gifu, Japan

- 3 "Synthesis and Photoluminescence Property of ZnO Microtubes" (Oral)

Liwei Lin, Hideo Watanabe, Masayoshi Fuji and Minoru Takahashi

The 9th International Symposium on Ceramic Materials and Components for Energy and Environmental Applications (2008CMCEE)

Sep. 10-14, 2008, Shanghai, China

2007

- 1 "Synthesis and Characterization of ZnO Microtubes" (Oral)

Liwei Lin, Masayoshi Fuji*, Takeshi Endo, Hideo Watanabe, Xiaowei Wang and Minoru Takahashi

Third Asian Particle Technology Symposium (ATP 2007)

Sep. 3rd-5th, 2007, Beijing, China

2 “A FACILE METHOD TO SYNTHESIZE ZnO MICROTUBES BY INVOLVING AMMONIA BUBBLES” (Poster)

Liwei Lin, Masayoshi Fuji, Takeshi Endo, and Minoru Takahashi

Asia Young Ceramist Conference in Tokai (AYCeCT 2007)

Jun.28th-29th, 2007, Shizuoka

3 “Synthesis and Characterization of Hexagonal Tubular ZnO” (Oral)

Liwei Lin, Masayoshi Fuji, Takeshi Endo, Hideo Watanabe, Xiaowei Wang and Minoru Takahashi

20st Fall Meeting of the Ceramic Society of Japan

Sep. 12-14, 2007, Nagoya, Japan

2006

1 “A FACILE METHOD TO SYNTHESIZE ZNO TUBES BY INVOLVING AMMONIA BUBBLES” (Poster)

Liwei Lin, Yongsheng Han, Masayoshi Fuji, Takeshi Endo, Hideo Watanabe and Minoru Takahashi

The second international conference on the characterization and control of interfaces for high quality advanced materials (ICCCI2006)

Sept. 6-9, 2006, Kurashiki, Japan

2 “Effect of pH on Synthesis of Single Crystalline ZnO Tubes” (Poster)

Liwei Lin, Yongsheng Han, Masayoshi Fuji, Takeshi Endo and Minoru Takahashi

Asia Young Ceramist Conference in Tokai (AYCeCT2006)

Oct.26-28, 2006, Tokai, Japan

3 “BUBBLE TEMPLATE METHOD FOR SYNTHESIS OF ZINC OXIDE TUBES” (Poster)

Liwei Lin, Yongsheng Han, Masayoshi Fuji, Takeshi Endo and Minoru Takahashi

International Workshop on Advanced Ceramics (IWAC2006)

Oct. 30– Nov. 3, 2006, Nagoya, Japan

ACKNOWLEDGEMENT

I can not believe I am sitting here writing acknowledge of my doctoral dissertation. This dissertation would not survive without the expert guidance and kind helps. In fact, I can think of enough people to fill another chapter, but I will try to keep it brief.

At first, I would like to express my appreciation to my supervisor – Prof. Masayoshi Fuji for his aborative guidance, elaborate discussions and valuable suggestions, and kind helps on my living in Japan. I also thank him for providing the environment where I can design and carry out my research on my own, write up research papers.

I would like to express my gratitude to Prof. Minoru Takahashi, executive director of Nagoya Institute of Technology, for the opportunity to carry out this work and his support and encouragement to the success of this work. I respect him deeply for his comprehensive academic knowledge. I will always keep his word in mind - “I will be the best in my field”.

I have to mention my real friends - Dr. Yongsheng Han and Ms. Chika Takai. It was so luck to meet them and their family in Japan. Thank Dr. Han for his helps during the starting of my study and the comments on my thesis. Thank Ms. Chika Takai for skillfully teaching me how to prepare TEM samples. I also own my sincere gratitude to my friend Ms. Chunxi Hai for sharing the dormitory with me during the last half of PhD

experience.

I also would like to thank all post doctoral researchers and all colleagues in CRL (Ceramics Research Laboratory) for their supporting and all secretariats for their kindly help. Especially, I would like to appreciate Dr. Takeshi Endo, Dr. Hideo Watanabe, Dr. Xiaowei Wang, and Dr. Takashi Shirai for their discussions and guided comments on my research works. I am grateful to Ms. Hisako Uchiyama, for her much kind helps in my living in Japan. I am also thankful to Mr. Kato, Mr. Seiji Yamashita and Mr. Kawade for their kind helps during the course of my thesis. The PhD experience is memorable, despite it is very hard, I met different undergraduate and graduate students, post doctors and staffs in the lab. During these three years, different people come, and different people leave, with different stories and mixed feelings, I really enjoy it.

Finally, I would like to express the best appreciations to my parents, my husband, and my younger brother. Their unconditional supports are gifts I treasure.

Liwei Lin